INFECTION AND IMMUNITY, May 2004, p. 2922–2938 Vol. 72, No. 5
0019-9567/04/$08.00+0 DOI: 10.1128/IAI.72.5.2922–2938.2004

Proteus mirabilis Genes That Contribute to Pathogenesis of Urinary Tract Infection: Identification of 25 Signature-Tagged Mutants Attenuated at Least 100-Fold

Laurel S. Burall,[1]† Janette M. Harro,[1]† Xin Li,[1] C. Virginia Lockatell,[2] Stephanie D. Himpsl,[1] J. Richard Hebel,[3] David E. Johnson,[2,4] and Harry L. T. Mobley[1]*

Department of Microbiology and Immunology,[1] Division of Infectious Diseases,[2] and Department of Epidemiology,[3] University of Maryland School of Medicine, and Research Service, Department of Veteran Affairs,[4] Baltimore, Maryland 21201

Received 2 October 2003/Returned for modification 11 December 2003/Accepted 26 January 2004

***Proteus mirabilis*, a common cause of urinary tract infections (UTI) in individuals with functional or structural abnormalities or with long-term catheterization, forms bladder and kidney stones as a consequence of urease-mediated urea hydrolysis. Known virulence factors, besides urease, are hemolysin, fimbriae, metalloproteases, and flagella. In this study we utilized the CBA mouse model of ascending UTI to evaluate the colonization of mutants of *P. mirabilis* HI4320 that were generated by signature-tagged mutagenesis. By performing primary screening of 2,088 *P. mirabilis* transposon mutants, we identified 502 mutants that ranged from slightly attenuated to unrecoverable. Secondary screening of these mutants revealed that 114 transposon mutants were reproducibly attenuated. Cochallenge of 84 of these single mutants with the parent strain in the mouse model resulted in identification of 37 consistently out-competed *P. mirabilis* transposon mutants, 25 of which were out-competed >100-fold for colonization of the bladder and/or kidneys by the parent strain. We determined the sequence flanking the site of transposon insertion in 29 attenuated mutants and identified genes affecting motility, iron acquisition, transcriptional regulation, phosphate transport, urease activity, cell surface structure, and key metabolic pathways as requirements for *P. mirabilis* infection of the urinary tract. Two mutations localized to a ~42-kb plasmid present in the parent strain, suggesting that the plasmid is important for colonization. Isolation of disrupted genes encoding proteins with homologies to known bacterial virulence factors, especially the urease accessory protein UreF and the disulfide formation protein DsbA, showed that the CBA mouse model and mutant pools are a reliable source of attenuated mutants with mutations in virulence genes.**

Proteus mirabilis, a gram-negative enteric bacterium, occurs as vegetative swimmer cells and hyperflagellated swarmer cells (6). Individuals suffering from urinary tract infections (UTI) caused by *P. mirabilis* often develop bacteriuria, kidney and bladder stones, catheter obstruction due to stone encrustation, acute pyelonephritis, and fever (40, 55, 60). *P. mirabilis* is one of the most common causes of UTI in individuals with long-term indwelling catheters, complicated UTI, and bacteremia among the elderly (57, 60). As the aging population expands, more individuals will be at risk for *P. mirabilis* UTI (87).

These infections of the urinary tract occur in an ascending manner (3). Uropathogenic microorganisms contaminate the periurethral area, enter the bladder through the urethra, and establish an initial colony. These bacteria have specific adhesion and motility phenotypes that allow them to ascend to the bladder against the flow of urine, which normally prevents bacterial invasion at low infectious doses. After initial colonization, *P. mirabilis* ascends the ureters and initiates an interaction with epithelial cells of the renal pelvis, which allows colonization of the kidney (38). In some cases, bacteria breach the one-cell-thick renal tubular epithelial barrier and enter the bloodstream (22).

The persistence of a *P. mirabilis* infection is compounded by the ability of this organism to cause the formation of urinary stones and encrust indwelling catheters (60), which provide a niche protected from host immune cells and antimicrobial agents. Indeed, the formation of stones around the organisms can make antibiotic treatment ineffective, since antibiotics must penetrate the stones to act. In addition, there have been reports of cephalosporin resistance in this species (12, 55, 67). Stone formation requires urease, which catalyzes the hydrolysis of urea into carbon dioxide and ammonia (40, 42, 49). An increased ammonium concentration raises the environmental pH, which mediates precipitation of normally soluble polyvalent ions from the urine (30). Specifically, precipitation of magnesium, ammonium, phosphate, and calcium ions results in formation of the struvite and carbonate hydroxyapatite crystals that comprise urinary stones (29).

Other virulence factors of *P. mirabilis* besides urease include hemolysin, flagella, fimbriae, and two proteases (55, 56, 59, 84, 93). Each of these virulence factors produces an easily identifiable phenotype in vitro that has been used to predict its role in pathogenesis and enables its identification. However, other virulence factors, such as transcriptional regulators, metabolic enzymes, stress response genes, and signal transducers, may be more difficult to identify since they may not be active in vitro or

* Corresponding author. Mailing address: Department of Microbiology and Immunology, University of Maryland School of Medicine, 655 W. Baltimore St., Baltimore, MD 21201. Phone: (410) 706-1617. Fax: (410) 706-6751. E-mail: hmobley@umaryland.edu.

† L.S.B. and J.M.H contributed equally to this study.

may produce only subtle or undetectable phenotypes in vitro. Several techniques have been developed to identify such virulence factors by in vivo screening, reducing the need for in vitro identification of potentially attenuated mutants; one of these techniques is signature-tagged mutagenesis (STM), which identifies attenuated mutants in pools of random transposon mutants following passage through an animal model (33). To adapt this method to a specific animal model, several limitations must be taken into account when virulence factors are screened for, including pool complexity and *trans* complementation of mutants by other mutant strains in the pool (66). However, STM has been successfully used to identify new virulence factors in several organisms, including *Salmonella enterica* serovar Typhimurium, *Legionella pneumophila*, *Escherichia coli*, *Klebsiella pneumoniae*, *Streptococcus pneumoniae*, and *Staphylococcus aureus* (20, 33, 50, 52, 70, 80). Preliminary application of STM to *P. mirabilis* led to identification of two virulence factors, a protease and *rpoN*-associated genes (93). Identification of additional *P. mirabilis* virulence factors would increase our understanding of how this organism infects and colonizes the bladder, ascends the ureters, and establishes infection in the kidneys.

We used STM of uropathogenic *P. mirabilis* in conjunction with the well-established murine model of ascending UTI to identify virulence determinants required for colonization of the urinary tract. STM relies on an ability to label each mutant within a large pool of mutants with a unique signature tag; the absence of a signature tag in the pool of mutants recovered from an experimental animal model indicates that a specific mutant is less fit and is out-competed in the host. An adaptation (39) of the CBA mouse model of ascending UTI, originally developed by Hagberg et al. (31), employs female mice, allows bladder inoculation, requires no obstruction, and, in our hands, has minimal vesicoureteral reflux. This model has been used for numerous investigations of *P. mirabilis* virulence determinants (11) and can be used to differentiate between nonpathogenic fecal strains and uropathogenic strains of *E. coli* capable of causing cystitis and acute pyelonephritis in humans.

Here we report identification of novel virulence determinant genes affecting motility, iron acquisition, transcriptional regulation, phosphate transport, urease activity, cell surface structure, and key metabolic pathways. These genes were localized to both the chromosome and a large plasmid.

MATERIALS AND METHODS

Bacterial strains, plasmids, and growth media. *P. mirabilis* HI4320 (Tet^r), a strain isolated from an elderly woman with urinary catheter-associated bacteriuria, was used as the recipient strain for transposon mutagenesis (60, 87). Forty-eight *E. coli* S17 λpir(pUT/mini-Tn*5*) (Kan^r Amp^r) strains, each with a uniquely tagged pUT/mini-Tn*5* sequence, were selected as the donor strains for conjugation with *P. mirabilis* HI4320. Plasmid clones used for identification of mutants were maintained in either *E. coli* DH5α [*supE44* Δ*lacU169* (Φ80*lacZ*ΔM15) *hsdR17 recA1 encA1 gyrA96 thi-1 relA1*] or *E. coli* VCS257 [*tyr258 supE44 glnV44 lacY1 dapD8 tonA53* Δ(*gal-UVRB*)*47 supF58 gyrA29 hsdS3* Δ(*thrA57*)*1*].

Nonswarming medium (10 g of tryptone per liter, 5 g of yeast extract per liter, 0.4 g of NaCl per liter, 5 ml of glycerol per liter, 15 g of agar per liter) was used to maintain the *P. mirabilis* transposon mutants and to prevent swarming on agar (7). Luria broth (10 g of tryptone per liter, 5 g of yeast extract per liter, 10 g of NaCl per liter) was routinely used to culture bacteria. Minimal A medium for *P. mirabilis* [10.5 g of K_2HPO_4 per liter, 4.5 of g KH_2PO_4 per liter, 0.47 g of sodium citrate per liter, 1 g of $(NH_4)_2SO_4$ per liter, 1 ml of 1 M $MgSO_4$ per liter, 10 ml of 20% glycerol per liter, 1 ml of 1% nicotinic acid per liter] was used for detection of auxotrophic *P. mirabilis* mutants (2). Swarming agar for *P. mirabilis* (10 g of tryptone per liter, 5 g of yeast extract per liter, 10 g of NaCl per liter, 15 g of agar per liter) was used for detection of an abnormal swarming phenotype in *P. mirabilis* mutants compared to the swarming phenotype of parental strain HI4320. Modified urea segregation agar, a combination of component A (4 g of tryptone, 4 g of yeast extract, 0.34 g of NaH_2PO_4, 1.03 g of Na_2HPO_4, 1 g of gelatin, 5 g of NaCl, 0.9 g of KH_2PO_4, 1.10 g of K_2HPO_4, and 15 g of agar in 900 ml of distilled H_2O, sterilized by autoclaving) and component B (9 g of D-glucose, 6 g of urea, and 0.035 g of phenol red in 100 ml of distilled H_2O, sterilized by filtration), was used for detection of urease activity in the *P. mirabilis* mutants (34). Iron-limiting medium was made by adding 0.33 mM 2,2-dipyridyl to Luria broth. Antibiotics were included at the following concentrations: kanamycin, 25 or 50 μg/ml; tetracycline, 15 μg/ml; and ampicillin, 100 μg/ml.

Construction of *P.mirabilis* HI4320 signature-tagged mutant library. The technique of Hensel et al. (33) was modified to screen *P. mirabilis* for virulence determinants. Isolates of *E. coli* S17 λpir, transformed with each of 48 pUT/mini-Tn*5*Km2 plasmids carrying random signature tags (Kan^r Amp^r) provided by C. Tang as described previously (93), were screened and selected for non-cross-reactivity of the signature tags. Overnight cultures of each donor strain and *P. mirabilis* HI4320 (Tet^r) were mixed 1:1 in a 96-well plate and transferred to 0.2-μm-pore-size membranes. The membranes were overlaid onto plain Luria agar plates and incubated at 37°C for 1 h to minimize replication of siblings. The filters were washed with phosphate-buffered saline (PBS), and the bacteria collected were plated on antibiotic-containing selective nonswarming agar plates (50 μg of kanamycin per ml, 15 μg of tetracycline per ml) and incubated overnight at 37°C to confirm transposon insertion. Transconjugants were screened for susceptibility to ampicillin (100 μg/ml) to confirm loss of the pUT plasmid. Multiple colonies from each conjugation reaction were selected for development of multiple screening pools. Forty-five pools of 48 mutants, including a negative control (a total of 2,088 tagged mutants), were assembled from the Tet^r Kan^r Amp^s transformants in 96-well plates, which were stored in microtiter plates at −80°C in 25% glycerol.

Southern and dot blot analyses. Random signature-tagged mutants of *P. mirabilis* HI4320 from conjugation trials were selected for Southern blot analysis to determine transposon insertion frequency and randomness. Chromosomal DNA isolated from *P. mirabilis* wild-type strain HI4320 and 10 transposon mutants were digested with HincII, XhoI, or EcoRI, gel electrophoresed on a 0.8 or 1% (wt/vol) agarose gel, and transferred onto Hybond-N+ membranes (Amersham Biosciences) (2). The membranes were probed with restriction fragments from within a transposon-kanamycin cassette isolated either by BamHI digestion (yielding a 1.7-kb fragment) or by EcoRI and XbaI digestion (yielding a 1.8-kb fragment) from the pUT/mini-Tn*5* vector. Probe labeling, hybridization, and detection were completed with the ECL direct nucleic acid labeling and detection system (Amersham Biosciences) by following the manufacturer's instructions. All of these mutants produced one or two bands that hybridized with the mini-Tn*5* probe, as expected since XhoI cut within the transposon. Four additional mutants, tested by digestion with EcoRI, which did not cut within the transposon, all produced only one band. All insertions were insertions in bands having a unique size, suggesting that transposon insertion occurred at random sites and only single insertions occurred (data not shown).

Additionally, we observed that multiple mutants that survived the primary screening and the secondary screening (see Results) were derived from the same conjugation and had identical signature tags. The isolation of multiple, identically tagged mutants raised the possibility that bacterial replication occurred during the 60-min conjugation period and that we were detecting identical daughter bacteria from different pools. Chromosomal DNA isolated from seven of these STM mutants with the signature-tagged transposon identified as D6 were digested with HincII, and a Southern blot was probed with a 1.7-kb BamHI fragment isolated from the pUT/mini-Tn*5*Km2 construct. Southern blot analysis showed that the seven *P. mirabilis* mutants had transposon insertions in different HincII fragments within the *P. mirabilis* genome; therefore, each mutant represented a distinct insertional event that resulted in a different inactivated gene (Fig. 1A).

Finally, *P. mirabilis* plasmid and chromosomal DNA preparations from attenuated mutants and the wild-type parental strain were spotted onto a Hybond+ membrane. The membrane was probed with the mini-Tn*5* transposon, as described above, to determine whether the transposon inserted into the plasmid or the chromosome.

Experimental CBA murine model of UTI. A modification (40) of the CBA mouse model of ascending UTI (31) was used to screen pools of 48 *P. mirabilis* STM mutants and for cochallenge competition assays performed with individual, putatively attenuated mutants and the parental strain *P. mirabilis* HI4320. Five female CBA/J mice (Harlen Sprague Dawley, Indianapolis, Ind.) that were 6 to

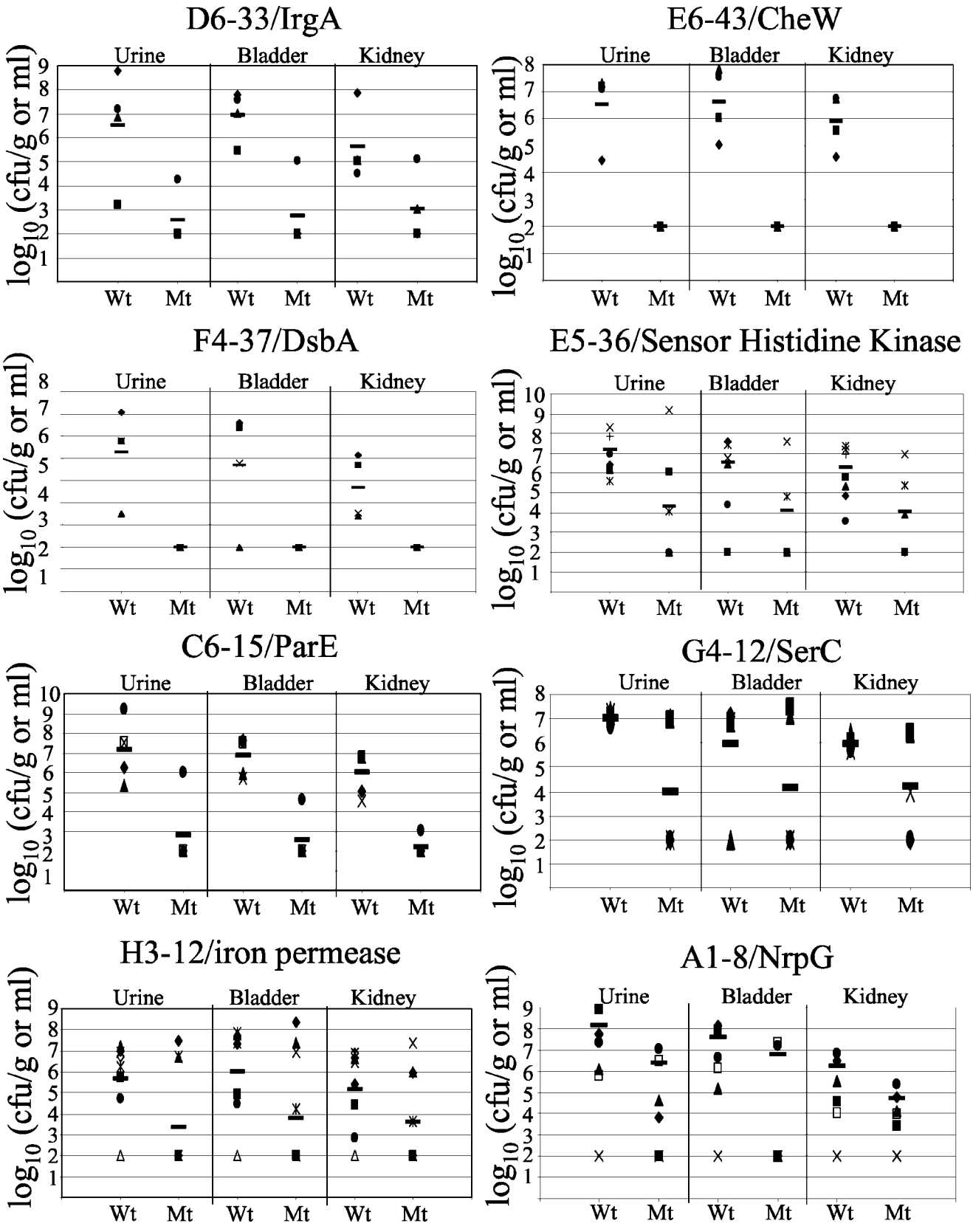

FIG. 1. Quantitative culture of in vivo cochallenges with selected attenuated mutants which were characterized phenotypically. Different symbols indicate different mice. The solid bars indicate the geometric means. See Table 1 for *P* values for each comparison. Wt, wild type; Mt, mutant.

8 weeks old were anesthetized with pentobarbital and inoculated with 5×10^7 CFU of each *P. mirabilis* STM pool (combined overnight culture of 48 mutants, grown separately in the wells of a microtiter plate) in 50 μl by insertion of a polyethylene catheter into the bladder through the urethra. A 1-ml sample of the inoculum (input pool) was standardized for optical density at 600 nm, and centrifuged pellets were stored at −20°C. After 4 days, the mice were sacrificed by administration of an overdose of isoflurane. The bladder and kidneys were removed and homogenized in PBS (8 g of NaCl per liter, 0.2 g of KCl per liter, 1.44 g of Na_2HPO_4 per liter, 0.24 g of KH_2PO_4 per liter; pH 7.2). The homogenized tissue samples were plated on NS agar containing tetracycline (40 μg/ml) and kanamycin (25 μg/ml) and incubated overnight at 37°C. After incubation, bacteria were washed from the plates with PBS (pH 7.2), and the optical density at 600 nm was standardized. Equivalent amounts of bacteria recovered from all bladder samples representing a single STM pool were combined to generate 1 ml of combined culture; the same procedure was repeated for the kidney samples. The output bladder and kidney samples were centrifuged, and the pellets were frozen at −20°C.

Cochallenge competition experiments were conducted by inoculating five female mice with 5×10^7 CFU of a 1:1 suspension of a *P. mirabilis* STM mutant (Kan^r) and *P. mirabilis* parental strain HI4320. The mice were sacrificed 7 days postinoculation, and samples of the urine, bladder, and kidneys were collected and weighed. Homogenized bladder and kidney samples were plated with a spiral plater onto NS agar containing no antibiotics and NS agar containing kanamycin (50 μg/ml). Viable counts from the plates were expressed in CFU per milliliter of urine or CFU per gram of tissue. Viable counts from the kanamycin-containing NS agar plates represented the exact counts for the *P. mirabilis* mutant. The wild-type counts were calculated by subtracting the mutant viable counts (based on the data obtained with the kanamycin-containing plates) from the viable counts for the NS agar plates with no antibiotic. The limit of detection for this technique was 10^2 CFU/ml of urine or 10^2 CFU/g of tissue; therefore, samples with no colonies were scored as having this value for the sake of statistical analysis. Data are expressed below as the ratio of the number of CFU of the mutant strain to the number of CFU of the wild-type strain recovered from urine, bladder, or kidney.

Statistical analysis. For cochallenge data, input numbers of CFU per milliliter and output numbers of CFU per milliliter of urine and numbers of CFU per gram of bladder and kidney were determined for both wild-type and mutant strains and statistically analyzed by using a repeated measure analysis of variance with rank order data (STATA software; Stata Co., College Station, Tex.) to determine whether there was a significant reduction in the mutant counts compared to the wild-type counts (4). Rank order data were used to prevent extreme outliers from skewing the analysis (4).

Labeling and hybridization screening of STM mutants. The standardized output bladder and kidney samples (each representing multiple mice inoculated with a single STM pool) were suspended in 100 μl of PBS and boiled for 5 min. A sample (2.5 μl) of a 1:10 dilution was used as the template for PCR I amplification of the variable tag (as described by Hensel et al. [33]) with Taq polymerase (Roche). The PCR conditions were 95°C for 4 min, followed by 20 cycles of 95°C for 30 s, 50°C for 45 s, and 72°C for 10 s and a final elongation step consisting of 72°C for 1 min. PCR I and PCR II primers P2 (5′ TACCTACAA CCTCAAGCT 3′) and P4 (5′TACCCATTCTAACCAAGC 3′) were complementary to the invariable regions flanking the variable sequence. The PCR I mixture was directly loaded on a 1.2% (wt/vol) SeaPlaque agarose gel (Cambrex), and after electrophoresis the amplified 80-bp fragment was isolated from the gel. A 2.5-μl sample of the gel slice was used as the template for PCR II (25 μl). For PCR II amplification we utilized a PCR digoxigenin (DIG) probe synthesis kit (Roche) according to the manufacturer's specifications to incorporate DIG-labeled dUTP into the amplified variable tag. The PCR II conditions and primers were identical to those of PCR I. A 10-μl sample of the PCR II DIG-labeled fragments was suspended in EasyHyb solution (Roche) and hybridized overnight with DNA dot blots in accordance with the manufacturer's instructions. Dot blots were created by using plasmid DNA extracted from the 48 pUT/mini-Tn*5* strains with a QIAprep Spin kit (Qiagen). Plasmid DNA (4.5 μl of a QIAprep preparation) was denatured with 0.4 M NaOH and blotted onto prewetted Hybond-N+ (Amersham Biosciences) by using a Bio-Dot microfiltration apparatus (Bio-Rad). DNA was cross-linked by baking membranes at 80°C for 2 h. After overnight hybridization, washing and blocking steps were completed by using a DIG wash and block buffer set (Roche) according to the manufacturer's specifications (except that in some instances, the wash temperature was adjusted to 54°C). After the blocking step, a 1:10,000 dilution of the anti-DIG-alkaline phosphatase (AP) Fab fragment (Roche) in blocking solution was applied to the membranes for 1 h. Excess antibody was removed with final washing steps in accordance with the manufacturer's specifications. Detection of the DIG-labeled fragments was completed by addition of the enzymatic substrate of alkaline phosphatase, CSPD (Roche), according to the instructions of the manufacturer.

Molecular cloning, arbitrary primed PCR, and sequencing. Sites of transposon insertion were assessed by several methods. Some transposon insertion sites were identified by cloning restriction fragments, obtained by digestion with EcoRI, MscI, EcoRV, or ApaI, into pBS (KS-). The resulting constructs were transformed into *E. coli* DH5α and selected on Luria agar containing kanamycin (50 μg/ml) and ampicillin (100 μg/ml). Other sites were amplified by arbitrary primed PCR, as described by Bahrani-Mougeot et al. (4), and ligated into pCR-BluntII. Arbitrary primed PCR was conducted in two sequential amplification steps with primers complementary to mini-Tn*5* ends reading outward and arbitrarily designed primers reading inward from the unknown sequence. For arbitrary PCR 1 we used primer Arb-1 (5′ GGCCACGCGTCGACTAGTCA NNNNN 3′) paired with primer 1957 (I end of mini-Tn*5*/variable end; 5′ GGT CATTAAACGCGTATTCA 3′) or primer 1955 (O end of mini-Tn*5*/transposon end; 5′ CAGGGCTTTATTGATTCCAT 3′). For this arbitrary primed PCR, a single *P. mirabilis* mutant colony, suspended in 30 μl of H_2O, was boiled and used as the template in a reaction with Taq DNA polymerase (Roche) according to the manufacturer's directions. After the initial denaturation for 5 min at 95°C, the thermocycler was programmed for 29 cycles with the following conditions: 95°C for 30 s, variable annealing (50 to 58°C) for 30 s, and 72°C for 90 s. The reaction was completed with a final elongation step consisting of 72°C for 5 min. For arbitrary PCR 2, the reagents and conditions were the same except that the template was a 2-μl sample from PCR 1 and different primer sets were used. For arbitrary PCR 2 we used primers complementary to sequences nested outside the PCR 1 primers, including primer 1956 (I end/variable end; 5′ CAGGGCTTTA TTGATTCCAT 3′) or primer 1954 (O end/transposon end; 5′ ACAGCCGGA TCCTCTAGAGT 3′) paired with Arb-2 (5′ GGCCACGCGTCGACTAGTCA 3′), which is the constant region of primer Arb-1. Arbitrary PCR 2 products were electrophoresed on a 1% (wt/vol) agarose gel, and bright bands were excised and eluted from the gel with a QIAquick gel extraction kit (Qiagen). The sizes of the arbitrary PCR fragments isolated ranged from 300 bp to 1.4 kb. To complete the sequencing of arbitrary PCR products, we used an automated sequencer (model 373; Applied Biosystems) and a PRISM Ready Reaction dye deoxy termination kit (Applied Biosystems).

All other mutations were isolated by cloning Sau3AI partial digests of chromosomal DNA from attenuated mutants into pHC79. The constructs were packaged by using Gigapack Plus (Stratagene) and were transformed into *E. coli* VCS257. Transformants were plated on Luria agar containing kanamycin (50 μg/ml) and ampicillin (100 μg/ml). Constructs in pBS were sequenced by using transposon-derived primer P7 (33) or vector primers T7 and T3, depending on the insert size. Constructs in pCR were sequenced by using universal forward and universal reverse primers. Constructs in pHC79 were sequenced from the P7 primer. Sequencing reactions were performed as previously described (93).

Sequence analysis. Sequence analysis and translation were done with online search engines at http://www.expasy.org. Homology searches of nucleotide and protein sequences were completed by using the public database provided in BLASTn, BLASTp, and BLASTx at http://www.ncbi.nlm.nih.gov. In addition, the nucleotide sequences of 13 mutants were queried in the Pathogenome database licensed by Compugen, which contained a nonpublic *P. mirabilis* genome. Compugen has since discontinued the Pathogenome database service, which provided database access to perform free queries and access to open reading frames (ORF) of homologous sequences for payment.

In vitro STM screening. To rule out the possibility that mutants were attenuated in the mouse model due to minor growth defects, STM screening was also used to test putative attenuated mutants for the ability to survive in vitro passage. Mutants that were identified as attenuated in vivo during previous STM screening with the mouse model were assembled into seven pools of 9 to 15 mutants. The mutants were cultured individually overnight, as described above, and then pooled. Each pooled bacterial suspension was then used to inoculate four culture tubes containing 5 ml of Luria broth supplemented with kanamycin (50 μg/ml) and tetracycline (15 μg/ml). A sample of the input inoculum was frozen at −20°C. Cultures were passaged twice each day (1:50 for the first passage and 1:500 for the second passage). After 4 days of culture, a sample (250 μl) was taken from each of the four cultures, and the samples were pooled for further processing as the output pool. The input and output samples were processed as described above for signature tag detection. This screening procedure was repeated by rearranging mutants into new pools that changed mutant groupings as much as possible in order to reduce the possibility of functional complementation between specific mutants. Mutants that failed to survive Luria broth passage were eliminated from the list of potential virulence genes.

The procedure described above was repeated by using minimal A medium (93)

for mutants identified as attenuated by cochallenge experiements. These mutants were assembled into six groups of 5 to 12 mutants and then cultured and pooled as described above. Bacteria in each suspension were harvested, washed, and resuspended in 500 μl of sterile distilled H_2O. Four culture tubes containing minimal A medium without antibiotics were inoculated with 100 μl of the suspension. Cultures were then passaged for 4 days and screened as described above.

Iron-limiting in vitro coculture. Tubes containing 3 ml of Luria broth containing 0.33 mM dipyridyl without a supplement or supplemented with 6 μl of 10 mM $FeSO_4$ (final concentration, 0.02 mM) or 6 μl of 8 mM hemin (final concentration, 0.016 mM) were inoculated with 30 μl of a 1:1 mixture of the wild type and mutant adjusted to an optical density at 600 nm 1.0, and they were passaged every 24 h. Two independent experiments were performed with four tubes for each condition and strain. Dilutions of the inoculum and culture obtained after 24 and 54 h of growth were plated on Luria agar and Luria agar containing kanamycin (50 μg/ml) to determine wild-type and mutant counts. Separate cultures of the wild type and A1-8 in Luria broth containing 0.33 mM dipyridyl were grown and passaged as described above, and dilutions were plated at 5, 24, 29, 53, and 72 h.

Plasmid restriction digests. *P. mirabilis* HI4320 and selected mutants were grown overnight in Luria broth supplemented with tetracycline (15 μg/ml); kanamycin (50 μg/ml) was added to the mutant cultures. Plasmids, isolated with a Mini Prep kit (Qiagen) and prewarmed EB buffer (Qiagen), were digested with AflII, DraI, EcoRV, MscI, NdeI, BglII, EcoRI, SpeI, PvuII, CvnI, HpaI, or ApaI, none of which cleaves within the transposon sequence. Digests were electrophoresed on 0.8% agarose gels and stained with ethidium bromide. A Southern blot was prepared and hybridized with a transposon-derived probe, as described above.

Sodium dodecyl sulfate- polyacrylamide gel electrophoresis and Western blotting. Suspensions of bacteria, normalized for optical density at 600 nm, were denatured for 5 min in sample buffer, electrophoresed through a sodium dodecyl sulfate–12% polyacrylamide gel, and transferred onto a polyvinylidene fluoride membrane (Immobilon-P; Millipore). Membranes were incubated with rabbit polyclonal antiserum against flagellin (56), MrpA (48), or UreC (32) and then incubated with a secondary goat anti-rabbit immunoglobulin conjugated to alkaline phosphatase. Membranes were developed with 5-bromo-4-chloro-3-indolylphosphate toluidinium (BCIP)-nitroblue tetrazolium as a substrate for the alkaline phosphatase. Confirming Western blotting was performed as described above except that the secondary antibody was coupled to horseradish peroxidase and blots were developed by using ECL.

Electron microscopy. One drop of a *P. mirabilis* stationary-phase culture (15 μl) was placed on a Formvar-coated grid for 5 min, and the excess liquid was wiped off. The grids were rinsed three times with distilled H_2O and stained with 1% sodium phosphotungstic acid (pH 6.8). The grids were examined with a JEM-1200EX II electron microscope (JEOL, Ltd., Tokyo, Japan).

RESULTS

***P. mirabilis* signature-tagged mutant pool assembly.** A *P. mirabilis* HI4320 library of 2,088 signature-tagged mutants was assembled by using transconjugants resulting from conjugations of wild-type *P. mirabilis* HI4320 with 47 *E. coli* S17 λpir (pUT/mini-Tn*5*Km2) strains. Each of the 47 transposon constructs had unique variable regions and was chosen because it was not cross-reactive with signature tags of other donor *E. coli* strains used for pool assembly. *P. mirabilis* transposon mutants were assembled into 45 screening pools containing 47 *P. mirabilis* transposon mutants, each derived from a uniquely tagged transposon, plus a negative control at filter coordinate D3. The negative control was a transposon mutant containing a signature tag that failed to hybridize and did not cross-hybridize with other tags.

Primary screening in CBA mice. Suspensions (50 μl) of bacteria from individual pools were transurethrally inoculated (total dose, 5×10^7 CFU [$\sim 10^6$ CFU of each mutant]) into the urinary bladders of five female CBA mice; at 4 day postinoculation, the mice were sacrificed. Bacteria recovered from the bladders and kidneys were separately pooled. We screened 2,088 *P. mirabilis* mutants in the CBA mouse model in 45 pools, isolated *P. mirabilis* from the bladder and kidney samples, and hybridized amplified, labeled tags from the inoculum (input) and recovered (output) samples with blots spotted with each of the 48 donor plasmids. For our initial screening, the characterization of mutants was broad; mutants were categorized as attenuated when a hybridization signal was absent, as having reduced intensity compared to the intensity of the input pool, or as having intensity equivalent to the intensity of the internal negative control. The initial screening yielded 502 *P. mirabilis* transposon mutants with a reduced ability to colonize the CBA mouse urinary tract during a 4-day infection.

Secondary screening in CBA mice. Nineteen secondary screening pools containing the 502 mutants were organized so that mutant pools had only single representation of the unique signature tags. In the secondary screening, 114 of the 502 transposon mutants were not recovered from the bladder or kidney samples or from both tissue samples.

Competitive cochallenge analysis to confirm attenuation. We tested 84 of the most attenuated of the 114 mutants in cochallenge experiments with wild-type *P. mirabilis* HI4320 in the CBA mouse model. Cochallenge experiments were conducted with a 1:1 inoculum of the mutant (Tet^r Kan^r) and the wild-type strain (Tet^r) (total inoculum, 5×10^7 CFU) in five mice. The length of the cochallenge experiments was increased from the 4 days used for screening pools to 7 days. The numbers of CFU of the wild type and mutants were determined for urine, bladder, and kidney samples, and a statistical analysis was performed to determine whether the ratios of the numbers of the mutant recovered to the numbers of the wild-type strain recovered were significantly different in these samples. A total of 37 mutants exhibited statistically significant attenuation and were selected for cloning and sequencing to identify the genes interrupted by the transposon. Twenty-five of 37 mutants were attenuated at least 100-fold in urine, bladder, or kidney samples (Table 1).

In vitro STM in rich culture medium. All 37 attenuated mutants were also screened by STM for the ability to survive 4 days of passage in vitro in Luria broth with antibiotic selection in pools of nine mutants. Of the 37 mutants tested, 5 were not recovered in this experiment (E5-36, F6-8, G1-43, G4-10, and H2-10), suggesting that there was a minor growth defect that prevented them from surviving in vitro Luria broth passage within pools. Three of these mutants (F6-8, G4-10, and H2-10) were not examined further, which left 34 mutants.

Identification of attenuated *P. mirabilis* mutants. The nucleotide sequences of 30 of the 34 *P. mirabilis* transposon mutants determined to be attenuated after primary and secondary screening and competitive cochallenge with wild-type HI4320 were determined by cloning chromosomal restriction fragments (7 mutants), by arbitrary PCR (18 mutants), and by cosmid cloning (5 mutants). The sequences of 11 *P. mirabilis* transposon mutants (A3-39, C1-18, C4-2, D5-9, D6-33, E5-36, F6-34, G1-43, G4-2, G4-12, and G5-30) were used to search the Pathogenome database (licensed by Compugen), which was a compilation of nonpublic genomes of pathogenic microorganisms which the user could search and use to determine the level of homology, the size of the ORF, and the organisms that were homologous to the nucleotide query. The sequence of each mutant had significant homology to a specific *P. mira-*

TABLE 1. Cochallenge with *P. mirabilis* H14320 and individual attenuated STM mutants in the CBA mouse model of ascending UTI[a]

Attenuated mutant	No. of mice	Mutant/wild type ratio (*P* value)[b]			
		Urine	Bladder	Kidney	Overall[c]
D6-33	4	6.3×10^{-7} (0.001)	5.3×10^{-6} (<0.001)	5.2×10^{-6} (0.051)	1.5×10^{-6} (<0.001)
G5-30	5	5.1×10^{-6} (<0.001)	3.1×10^{-6} (<0.001)	5.0×10^{-5} (<0.001)	5.5×10^{-6} (<0.001)
D6-26	13	9.9×10^{-7} (0.003)	2.4×10^{-5} (0.004)	6.8×10^{-5} (0.002)	2.8×10^{-6} (0.001)
H4-34	5	9.5×10^{-6} (0.007)	3.4×10^{-6} (0.007)	1.4×10^{-5} (<0.001)	6.4×10^{-6} (<0.001)
E6-43	4	8.0×10^{-6} (<0.001)	3.8×10^{-6} (<0.001)	3.6×10^{-5} (<0.001)	7.3×10^{-6} (<0.001)
E6-41	5	1.0×10^{-5} (<0.001)	4.1×10^{-6} (<0.001)	1.0×10^{-4} (<0.001)	6.9×10^{-6} (<0.001)
F6-34	3	4.6×10^{-6} (<0.001)	9.9×10^{-6} (<0.001)	2.7×10^{-5} (<0.001)	8.4×10^{-6} (<0.001)
D1-30	4	7.9×10^{-6} (<0.001)	6.7×10^{-6} (<0.001)	5.1×10^{-5} (<0.001)	1.0×10^{-5} (<0.001)
D2-41	5	NA (NS)[d]	7.0×10^{-6} (0.005)	4.7×10^{-4} (0.059)	9.6×10^{-6} (0.022)
F1-29	4	7.1×10^{-7} (0.021)	7.3×10^{-6} (<0.001)	7.3×10^{-4} (<0.001)	1.9×10^{-6} (<0.001)
F4-37	4	3.1×10^{-6} (<0.001)	6.3×10^{-6} (<0.001)	2.2×10^{-4} (<0.001)	6.2×10^{-6} (<0.001)
H2-10	5	6.8×10^{-6} (<0.001)	4.4×10^{-6} (<0.001)	3.7×10^{-5} (<0.001)	7.3×10^{-6} (<0.001)
A5-34	4	1.2×10^{-5} (0.001)	NA (NS)	3.2×10^{-5} (0.006)	6.6×10^{-6} (0.005)
E5-36	8	9.6×10^{-6} (0.001)	1.0×10^{-5} (0.017)	8.5×10^{-5} (<0.001)	1.4×10^{-5} (<0.001)
G1-43	5	1.0×10^{-5} (0.004)	1.6×10^{-5} (0.005)	2.0×10^{-5} (0.046)	1.4×10^{-5} (0.006)
A3-39	5	2.1×10^{-5} (<0.001)	1.7×10^{-5} (<0.001)	2.4×10^{-5} (<0.001)	2.0×10^{-5} (<0.001)
B6-40	3	1.7×10^{-5} (<0.001)	2.3×10^{-5} (<0.001)	7.3×10^{-5} (<0.001)	2.6×10^{-5} (<0.001)
G1-38	4	3.2×10^{-5} (<0.001)	3.5×10^{-5} (<0.001)	1.8×10^{-4} (0.014)	4.6×10^{-5} (<0.001)
C6-15	5	4.4×10^{-5} (<0.0001)	4.4×10^{-5} (<0.0001)	1.7×10^{-4} (<0.0001)	6.9×10^{-5} (<0.0001)
F6-8	5	4.8×10^{-5} (<0.001)	4.5×10^{-6} (<0.001)	6.0×10^{-4} (<0.001)	1.5×10^{-5} (<0.001)
G4-10	8	2.4×10^{-4} (0.01)	5.1×10^{-6} (<0.001)	6.1×10^{-3} (0.036)	1.5×10^{-5} (0.001)
C4-41	5	NA (NS)	5.1×10^{-4} (0.025)	8.2×10^{-4} (0.001)	6.0×10^{-4} (0.019)
G4-12	5	9.0×10^{-4} (0.003)	NA (NS)	NA (NS)	6.1×10^{-3} (0.022)
D6-39	3	NA (NS)	4.8×10^{-3} (<0.001)	2.6×10^{-3} (<0.001)	4.5×10^{-3} (0.001)
H3-12	8	4.9×10^{-3} (<0.0001)	6.0×10^{-3} (<0.0001)	2.6×10^{-2} (<0.0001)	9.2×10^{-3} (<0.0001)
B6-23	4	1.2×10^{-2} (<0.0001)	8.6×10^{-3} (0.007)	7.1×10^{-2} (0.013)	8.7×10^{-3} (<0.0001)
D5-9	9	5.1×10^{-3} (0.024)	NA (NS)	NA (NS)	3.0×10^{-2} (0.025)
B4-2	5	NA (NS)	5.9×10^{-3} (0.026)	3.7×10^{-2} (0.003)	1.4×10^{-2} (0.006)
A1-8	6	1.0×10^{-2} (0.033)	NS (NS)	1.1×10^{-1} (<0.0001)	1.9×10^{-2} (0.005)
B4-38	5	NA (NS)	NA (NS)	1.5×10^{-2} (0.002)	NA (NS)
C1-18	5	NA (NS)	2.8×10^{-2} (0.001)	NA (NS)	1.4×10^{-1} (0.012)
D4-8	5	1.4×10^{-1} (0.005)	3.1×10^{-1} (<0.0001)	3.3×10^{-2} (0.021)	1.1×10^{-1} (0.001)
C4-2	5	NA (NS)	5.9×10^{-2} (0.001)	5.9×10^{-2} (0.001)	1.5×10^{-1} (0.001)
C6-9	7	8.3×10^{-2} (0.01)	NA (NS)	NA (NS)	9.0×10^{-2} (0.024)
B2-22	4	NA (NS)	NA (NS)	1.9×10^{-1} (<0.0001)	NA (NS)
G4-2	4	NA (NS)	NA (NS)	5.6×10^{-1} (0.038)	NA (NS)
B2-9	10	7.7×10^{-1} (0.028)	NA (NS)	NA (NS)	NA (NS)

[a] Five mice were transurethrally inoculated with 10^7 CFU (approximately equal numbers of the parent strain and the mutant). After 7 days, the mice were sacrificed, and the numbers of CFU per gram or the numbers of CFU per milliliter were determined for the wild-type parent and mutant strains.

[b] Data for significantly attenuated mutants are expressed as the ratio of the number of mutant CFU per gram or the number of mutant CFU per milliliter to the number of wild-type parent strain CFU per gram or the number of wild-type parent strain CFU per milliliter. Statistically significant differences in the numbers of CFU were determined by the method described by Bahrani-Mougeot *et al*. (4).

[c] Overall *P* values were calculated like other *P* values were calculated, but all numbers were pooled without regard to tissue.

[d] NA, not applicable (ratios were not statistically significantly different from 1); NS, not statistically significant.

bilis ORF whose entire sequence was obtained. Sequences identified in the 30 STM mutants were compared to known sequences by BLASTX searches to identify homologs that could predict a function (Table 2). E values less than 0.05 were considered significant and were used to rank the homologies. One exception was made for a mutant (B2-9) that had no other homologs and only a short nucleotide sequence with which to search. The complete nucleotide sequences of 11 ORF and the partial nucleotide sequences of 19 other mutants were translated, and the protein sequences were analyzed by BLASTp. The BLASTp analysis revealed protein homologs for 30 sequenced transposon mutants, and putative gene identification was based on homology scores with the lowest E values (Table 2). Mutants were classified in several categories, including motility (*cheW*), iron acquisition (*hasR*, *nrpG*, *irgA*), plasmid encoded (*parE*, *pilX3*), transcriptional regulation (*hdfR*, two-component sensor kinase), phosphate transport (*pstC*, *pstS*), urease activity (*ureF*), cell surface structure (*dsbA*), and key metabolic pathways (*carA*, *asnC*).

Homologs in the uropathogenic *E.coli* CFT073 genome. STM mutant sequences were also compared by using BLASTX searches with the uropathogenic *E. coli* CFT073 genome (Table 2). Since uropathogenic *E. coli* CFT073 is the only closely related uropathogen whose entire genome sequence is known (90), we reasoned that homologs would likely be present in this strain. Of the 33 distinct *Proteus* genes, 24 had homologs in uropathogenic *E. coli* CFT073. These genes included genes for chemotaxis (*cheW*), assembly of surface structures and secreted proteins with disulfide bonds (*dsbA*), iron acquisition (*hasR*, *nrp*, *irgA*), transcriptional regulators (*hdfR*, two-component sensor kinase), and various metabolic enzymes.

Only 9 of the 33 identified genes had no homologs in the CFT073 genome. Urease (*ureF*) is a hallmark of uropathogenic *P. mirabilis* and is generally not found in uropathogenic *E. coli*

TABLE 2. Identification of homologs of products of disrupted genes in attenuated *P. mirabilis* STM mutants

Gene function	STM mutant attenuated in cochallenge	Tissue(s) in which mutant was significantly outcompeted by the wild type[a]	In vitro STM: growth in minimal medium[b]	Closest homolog[c]	Species and description	Homolog present in *E. coli* CFT073[d]
Urease	B6-40	All	+	UreF	*Proteus mirabilis* urease accessory protein UreF	−
Motility	E6-43	All	+	CheW	*Yersinia pestis* positive regulator of CheA; chemotaxis	+
Periplasmic protein folding	F4-37	All	+	DsbA	*Yersinia pestis* thiol:disulfide interchange protein	+
Iron acquisition	G4-2	Kidney	+	HasR	*Pasteurella multocida* membrane-bound heme receptor	+
	A1-8	Urine, kidney, overall	+	NrpG	*Proteus mirabilis nrp* operon; nonribosomal peptide synthesis; phosphopantetheinyl transferase	+
	H3-12	All	+		*Yersinia pestis* putative iron transport permease	−
	D6-33	All	+	IrgA	*Yersinia pestis* putative outer membrane protein IrgA	+
DNA binding regulatory proteins	C6-9	Urine, overall	+	SocE	*Myxococcus xanthus* stringent response regulator	+
	D5-9	Urine, overall	+	HdfR	*Yersinia pestis* regulator of FlhDC (master flagellar operon)	+
	C1-18	Bladder, overall	+	HdfR	*Yersinia pestis* regulator of FlhDC (master flagellar operon)	+
	E5-36[e]	All	−		*Yersinia pestis* two-component system sensor kinase	+
	E6-41	All	−	AsnC	*Yersinia pestis* regulatory protein for *asnA* and *gidA*	+
	F1-29	All	+	YhdG	*Proteus vulgaris* YhdG homolog	+
Plasmid encoded	C6-15	All	+	ParE	*Nitrosomonas europaea* plasmid stabilization factor	−
	C4-41	Bladder, kidney, overall	+	PilX3	*Escherichia coli* conjugative plasmid transfer	−
Cell envelope	B6-23	All	+	MrcA	*Salmonella enterica* serovar Typhimurium peptidoglycan synthetase	+
	B4-2	Bladder, kidney, overall	+		*Yersinia pestis* membrane heat shock protein	+
	D6-26	All	+		*Yersinia pestis* putative glycosylase	+
	F6-34	All	+		*Yersinia pestis* putative exported protein	+
	A3-39	All	+		*Yersinia pestis* putative exported protein	+
Transport	G1-43[e]	All	+	PstC	*Yersinia pestis* phosphate transport system permease	+
	H4-34	All	+	PstS	*Yersinia pestis* phosphate-binding periplasmic protein	+
Metabolic	B2-9	Urine	<	HemY	*Escherichia coli* late step of protoheme IX synthesis	Weak
	C4-2	Bladder, kidney, overall	+		*Plasmodium falciparum* putative chromosomal maintenance	Weak
	D4-8	All	−	CarA	*Escherichia coli* carbamoyl phosphate synthetase	+
	G4-12	Urine, overall	+	SerC	*Yersinia enterocolitica* 3-phosphoserine aminotransferase	+
	D6-39	Bladder, kidney, overall	+		*Yersinia pestis* anaerobic ribonucleoside triphosphate reductase	+
	G1-38	All	+		3-Deoxy-D-arabinoheptulosonate-7-phosphate synthase	+
Hypothetical	B2-22	Kidney	+		*Yersinia pestis* hypothetical gene	−
	G5-30	All	+		*Yersinia pestis* hypothetical protein	+
Unknown	A5-34	Urine, kidney, overall	+		Limited sequence, no hits	NA
	B4-38	Kidney	+		Limited sequence, no hits	NA
	D1-30	All	+		Limited sequence, no hits	NA
	D2-41	Urine, kidney, overall	+		Limited sequence, no hits	NA

[a] Following transurethral cochallenge of mice with wild-type and individual STM mutants, tissues in which there was a statistically significant reduction in the number of CFU per g or the number of CFU per milliliter for the STM mutant compared to the values for the wild-type strain. All, urine, bladder, and kidneys; overall, statistically significant reduction in the number of CFU of the mutant when data for each tissue were combined and tested for statistical significance.

[b] Groups of STM mutants were repeatedly passaged in minimal salts medium for 4 days. The resulting cultures were processed like the in vivo STM mutants. +, specific mutant present at the end of passage; <, mutant absent after passage but able to grow when it was cultured individually in minimal salts medium; −, mutant absent after passage and unable to grow when it was cultured individually in minimal salts medium.

[c] A nucleotide sequence (300 to 600 bp) from an ORF interrupted by Tn5 was used in a BLASTX analysis. The annotation of the best match is indicated. The E values were $\leq 6 \times 10^{-4}$ for all homologs except for B2-9, for which the E value was 1.5.

[d] The E value of the best match in *E. coli* CFT073 (pyelonephritogenic strain) was $\leq 5 \times 10^{-4}$ except for B2-9 (E value, 1.6) and C4-2 (E value, 0.79) (indicated as weak). +, CFT073 has a homolog; −, CFT073 does not have a homolog; N/A, no sequence available for search.

[e] Mutant that was out-competed during in vitro STM in Luria broth.

strains. Two genes related to plasmid maintenance and transfer (*parE* and *pilX3*) were found in *P. mirabilis* but not CFT073; this is not surprising since CFT073 does not carry a plasmid. The closest match for the first of these mutants, C6-15, with a proposed function was the *Nitrosomonas europaea* putative ParE plasmid stabilization protein, followed by the *Vibrio cholerae* ParE protein. PilX3 is an outer membrane protein involved in conjugative transfer of plasmids. Another mutant, H3-12, was most closely related to a *Yersinia pestis* putative iron transport permease, followed by the *Brucella melitensis* anguibactin permease; however, the gene had no matches in CFT073 within the first 100 hits. Finally, the B2-22 mutant had several hits to conserved hypothetical proteins, and the closest was in *Y. pestis*. The presence of a plasmid that is absent in *E. coli* CFT073 and its maintenance system, coupled with the distant relationship of the iron transport permease and the complete lack of a homolog for the B2-22 mutant, indicates that *P. mirabilis*, while sharing some pathogenic strategies with uropathogenic *E. coli*, has additional genes that mediate different pathways to colonize the urinary tract and cause damage to the host.

Use of minimal A medium for identification of auxotrophs and for in vitro STM. All STM mutants were cultured in minimal A medium to identify auxotrophic mutants. We isolated one mutant, E6-41, with a reduced capacity to grow on minimal A medium compared to the ability of wild-type strain HI4320. Mutant E6-41 was found to have AsnC, the positive regulator of *asnC*, *asnA*, and *gidA* (Table 2).

Additional STM screening was carried out to identify which mutants could not survive in vitro passage in minimal A medium for 4 days. This screening analysis was designed to identify mutants with minor metabolic defects that affected growth in nutrient-limiting conditions, as opposed to the in vitro screening analysis described above, in which we identified growth defects that affect survival in a nutrient-rich environment. Only two mutants, one encoding carbamoyl phosphate synthetase (VIII-D4) and one encoding the HemY homolog (IX-B2), were not recovered in this analysis (Table 2).

Assessment of *P.mirabilis* mutants for known virulence properties. We examined 16 of the 34 attenuated mutants for synthesis of *P. mirabilis* virulence factors, including flagella, fimbriae, and urease (Table 3). The mutants were chosen based upon in vitro phenotypic deficiencies and putative identification of the interrupted genes (Table 2). We analyzed the production of surface structures, including flagella and mannose-resistant *Proteus*-like fimbriae, with rabbit antiserum raised against flagellin and the MrpA subunit, respectively. Additionally, we screened some mutants with antibodies for the urease accessory protein, UreC. Using Western blot analysis with the flagellin antibody, we identified mutant E5-36, a mutant with a two-component system sensor kinase homolog, as a mutant that is negative for flagellin production (Fig. 2G); however, reverse transcription-PCR revealed the presence of a *flaA* transcript in this mutant (S. Heimer, unpublished data), and a Western blot on which a higher protein concentration was loaded revealed a band corresponding to flagellin. Thus, all mutants tested retained the ability to make flagellin protein; this included mutant F4-37 (the band on the Western blot was very faint; the band was confirmed to be present on a Western blot loaded with a larger amount of protein) with the DsbA homologue. Significantly, mutant F4-37 was the only mutant that was negative for the MrpA fimbrial subunit polypeptide (Table 3). Other studies have demonstrated the critical role of DsbA in the synthesis of bacterial fimbriae, suggesting that a mutant could lack other types of adhesive fimbriae as well; indeed, other fimbriae produced by *P. mirabilis*, the ambient temperature fimbriae, are also not assembled (data not shown).

TABLE 3. Phenotypes of signature-tagged mutants

Mutant	In vitro phenotype		Western analysis[c]	
	Swarming[a]	Urease[b]	Anti-FlaA	Anti-MrpA
A1-8	Aberrant	+	+	+
A3-39	Normal	+	+	+
B2-9	Aberrant	+	+	+
B6-23	Aberrant	+	+	+
B6-40	Normal	−[d]	ND[e]	ND
C6-15	Aberrant	+	+	+
D6-33	Normal	+	+	+
E5-36	Deficient	+	Weak	+
E6-41	Normal	+	+	+
F4-37	Aberrant	+	+	−
F6-34	Normal	+	+	+
G1-43	Normal	+	+	+
G4-12	Aberrant	+	+	+
G5-30	Aberrant	+	+	+
H3-12	Aberrant	+	+	+
H4-34	Normal	+	ND	ND

[a] Swarming pattern on Luria agar plate after 24 h. All attenuated mutants not listed swarmed normally.
[b] Presence of urease activity on urea segregation agar after 24 h.
[c] Western blots were prepared for detection of flagella, MR/P fimbriae, and urease as described in Materials and Methods.
[d] All strains, including B6-40, produced UreC, as detected by Western blotting.
[e] ND, not determined.

To identify urease-negative isolates, mutants were cultured on modified urea segregation agar. One mutant, B6-40, was deficient for urease enzymatic activity. Mutant B6-40 was found to contain an insertion in the gene encoding UreF, the accessory protein required for nickel incorporation into the urease apoenzyme, UreABC. A lack of this protein results in synthesis of an enzymatically inactive urease apoenzyme (35). Western analysis with the UreC antiserum revealed that this mutant, as well as all of the mutants tested, synthesized the UreC subunit. This was not surprising since *ureF* is downstream of *ureABC* in the urease gene cluster (43); therefore, it is predicted that this mutant could synthesize an inactive apoenzyme comprised in part of the UreC subunit.

Swarming phenotypes. STM mutants were examined for patterns of swarming differentiation on the surfaces of Luria agar plates, and the results were compared to the results for wild-type *P. mirabilis*. The swarming activities of 13 STM mutants (A1-8, B2-9, B6-23, C6-15, D6-26, E5-36, E6-43, F4-37, G4-12, G5-30, and H3-12) were deficient in terms of the number and length of the swarming rafts within the bull's-eye colonies on swarming agar compared to the results obtained for wild-type *P. mirabilis* strain HI4320; the patterns for five of these mutants are shown in Fig. 2B to F. In addition, *P. mirabilis* A1-8/*nrpG* had a dendritic swarming pattern, as shown in previous studies (26). Some of the phenotypes seen were a shorter swarming migration, hyperextended regions, and more

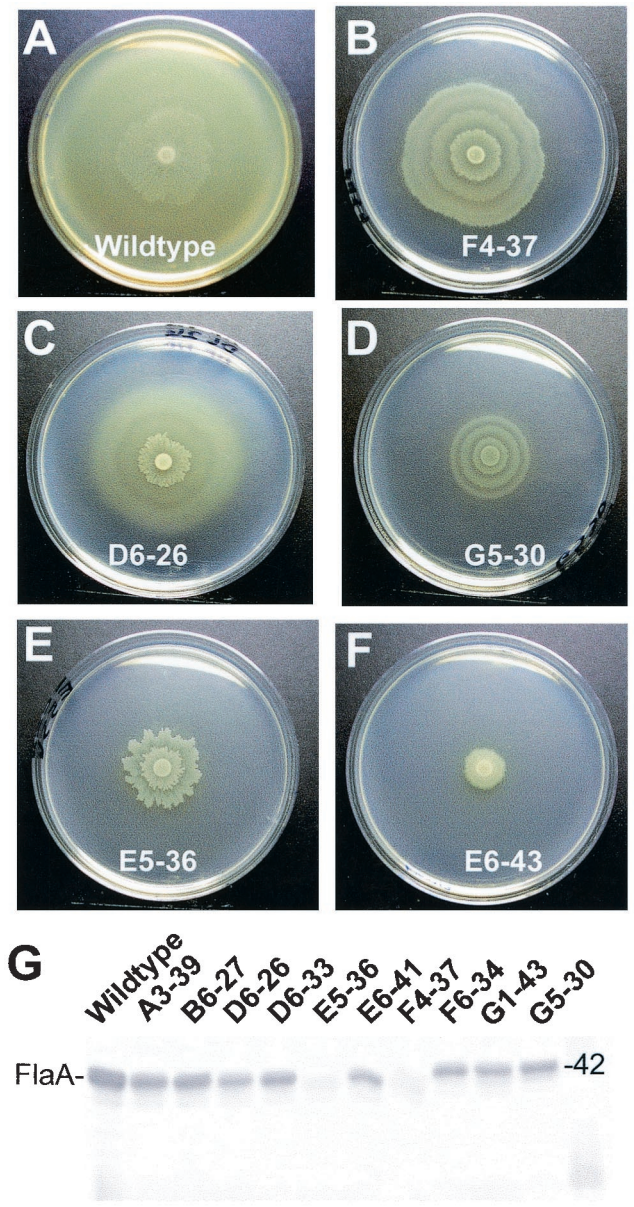

FIG. 2. Swarming differentiation and flagellum synthesis of *P. mirabilis* HI4320 (wild type) and STM mutants on agar. The wild-type strain (A) and selected mutants (B to F) were each spotted onto the center of a Luria agar plate and incubated for 16 h. The wild-type strain swarmed to the outer edge of the plate. The mutants displayed various patterns of aberrant swarming. (G) Western blot of whole-cell preparations of the wild-type strain and selected STM mutants reacted with rabbit anti-FlaA and developed as described in Materials and Methods. The number 42 indicates the electrophoretic mobility of a 42-kDa protein as estimated by using standard proteins. Mutant E5-36 appeared to be negative for flagellin production, and mutant F4-37 was faintly positive for flagellin production. An additional Western blot in which a higher concentration of total protein was used revealed the presence of flagellin in both mutants, although the amount was reduced.

transparent and irregular swarming, as in *P. mirabilis* C6-15/*parE* (Fig. 3). All mutants not discussed here consistently showed normal swarming phenotypes in all trials.

Polysaccharide synthesis. An analysis of mutant G5-30, a mutant with a mutation in the polysaccharide deacetylase homologue, included assessment of the cell surface structure of the mutant compared to that of wild-type *P. mirabilis* by electron microscopy. This mutant is abnormally short compared to wild-type strain HI4320, but the mutant appeared to retain the surface fimbrial and flagellar structures (data not shown).

Transposon localization. Dot blots (Fig. 3F) and Southern blots (data not shown) of the ~42-kb plasmid and chromosomal DNA isolated from each STM mutant were probed with the transposon to identify whether the insertions were in the plasmid or the chromosome. The transposon was found in the chromosome of 27 mutants, including the three unsequenced mutants. Two mutants, a putative plasmid stabilization factor mutant (C6-15/*parE*) and a PilX3 mutant (C4-41), however, carried the Tn*5* insertion within the ~42-kb plasmid of *P. mirabilis* HI4320 (Fig. 3F) (note that chromosomal DNA preparations also carried the plasmid). This suggested that at least two virulence genes may be carried on the plasmid and that the plasmid itself is required for full virulence.

Plasmid stabilization factor. *P. mirabilis* C6-15 (transposon insertion in the ~42-kb plasmid of *P. mirabilis* HI4320), a highly attenuated mutant (Table 1), had a distinct phenotype that was initially observed on nonswarming agar plates used for cochallenge counting (Fig. 3A). The colonies had a fried-egg appearance and were more translucent than wild-type colonies. Additionally, the swarming phenotype was aberrant, with growth that was more transparent and irregular with clear spots rather than opaque and evenly distributed throughout the swarming regions (Fig. 3B and C). Additional differences were observed during microscopic evaluations of Gram-stained preparations that showed that the cells of this mutant are shorter than the wild-type cells (0.72 ± 0.3 μm for the mutant and 1.13 ± 0.39 μm for the wild type; $P = 0.01$) (Fig. 3D and E). The corresponding mutation was found to be in a gene homologous to a *V. cholerae* gene encoding the plasmid stabilization factor, ParE.

Compared to the results of restriction mapping of the plasmid from the wild-type strain and another mutant (H3-12), restriction mapping of the plasmid isolated from mutant C6-15/*parE* revealed both new restriction sites outside the transposon insertion and apparent deletions and potential rearrangements, which were suggested by increases in the sizes of some bands that appeared to be greater than the sizes explained by the transposon (Fig. 4). For example, BglII digestion revealed a new band at 9.5 kb for mutant C6-15; the other bands remained at the same positions. The BglII digestion pattern suggests that there was a loss of DNA that was not apparent in the *Eco*RI digestion pattern, in which the total size was the same. This suggests that there was a rearrangement in the DNA within the plasmid, with the apparently missing DNA in the BglII digest potentially masked by a DNA band at the same position. The transposon was localized by Southern blotting to the shifted bands in DraI and HpaI digests and to the new band in the BglII digest. The transposon was also found in the 5-kb fragment of the EcoRI digest.

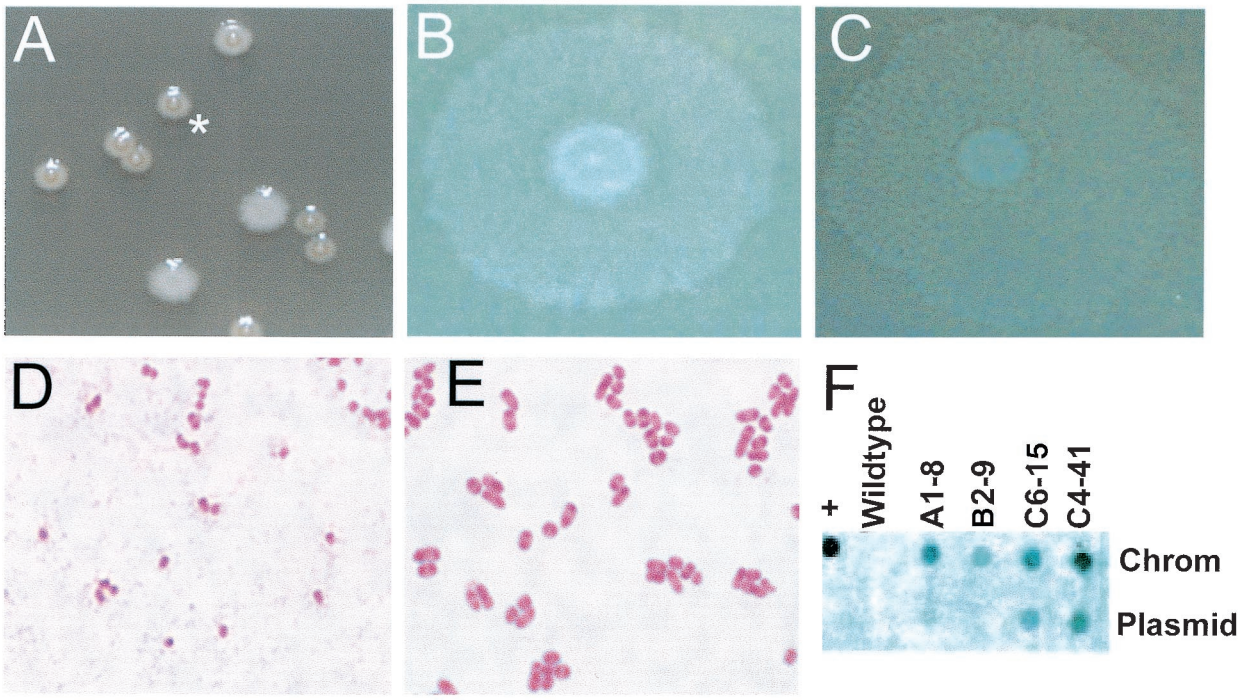

FIG. 3. Colony morphology and genomic localization of C6-15/*parE*. (A) Mixture of the *P. mirabilis* wild type and C6-15/*parE* (asterisk) plated on nonswarming agar and incubated overnight at 37°C. (B and C) *P. mirabilis* wild type (B) and C6-15/*parE* (C) spotted (5 μl) on swarming agar and incubated overnight. The *parE* mutant shows small clear zones within the swarm regions. (D and E) Micrographs of Gram-stained overnight cultures of *P. mirabilis* C6-15 (D) and *P. mirabilis* wild-type strain HI4320 (E) taken with a ×100 objective. The average length of wild-type cells was 1.13 μm, while the average length of mutant C6-15 cells was 0.72 μm ($P = 0.01$). (F) Plasmid and chromosomal DNA from STM mutants A1-8, B2-9, C4-41, and C6-15, as well as the *P. mirabilis* HI4320 parent strain and (as a positive control) plasmid pUTkm2, spotted on a separate filter. The membranes were probed with a 1.8-kb EcoRV-XbaI fragment of the mini-Tn*5*Km2 sequence. Chrom, chromosome.

Studies with iron acquisition homologs. To date, there have been only limited studies of iron acquisition in *Proteus* spp. (23, 26, 51). Based on homologies to genes encoding components of iron acquisition systems, three mutants, *P. mirabilis* G4-2/*hasR*, A1-8/*nrpG*, and H3-12/iron transport permease, were assayed for the ability to acquire heme, ferric iron, or ferrous iron from the growth medium. To identify a phenotype for these mutants, an in vitro coculture was used to apply increased selective pressure and potentially allow more subtle growth differences to be measured. No significant differences were seen under iron-limiting conditions without iron supplementation for any of the three mutant strains when the survival was compared to the wild-type survival on day 1 (Fig. 5). However, on day 2, the growth of both the *hasR* mutant (Fig. 5A) and the iron transport permease mutant (Fig. 5D) was significantly reduced under iron-limiting conditions compared to the growth of the wild type. The growth of the G4-2/*hasR* mutant was reduced by an average of 1.25-fold ($P = 0.002$). The growth of the iron transport permease mutant was reduced by nearly fourfold ($P < 0.0001$). The A1-8/*nrpG* mutant (Fig. 5B) showed no significant reduction in growth at any time under iron-limiting conditions during coculture, although this mutant tended to be out-competed an average of approximately fivefold ($P = 0.09$). However, because of the possibility that an *nrp* gene product could be secreted from the bacterium and thus complement a mutant's defect in coculture, separate iron-limiting cultures were grown, and the results showed that there was a significant reduction ($P < 0.001$) at 24 h but not at 5 h or any time thereafter (Fig. 5C). Iron supplementation with hemin or $FeSO_4$ restored the ability of the *hasR* and *nrpG* mutants to survive iron-limiting conditions. For the iron transport permease mutant, however, there were nearly significant reductions in bacterial counts on day 1 ($P = 0.053$). On days 2 and 3, the counts for this mutant were reduced by 0.5 log and nearly 5 logs ($P = 0.002$ and $P < 0.0001$, respectively) compared to the wild-type counts in a culture supplemented with $FeSO_4$ (Fig. 5E). Hemin supplementation also failed to recover survival of the iron transport permease mutant, which was reduced 0.5 and 4 logs on days 2 and 3, respectively ($P < 0.0001$ and $P = 0.023$, respectively) (Fig. 5F). Interestingly, this mutant was able to recover on day 3 when there was no supplementation under the iron-limiting conditions.

DISCUSSION

STM was used to identify virulence determinants of uropathogenic *P. mirabilis* in conjunction with a murine model of experimental UTI. Four sequential screening analyses of 2,088 mutants (primary screening, secondary screening, cochallenge, and in vitro STM in rich medium) were used to identify 34 attenuated mutants and 29 *P. mirabilis* genes involved in a wide variety of functions, including known virulence genes and genes for iron acquisition, transcriptional regulation, plasmid stability, capsule synthesis, and metabolism in the environment

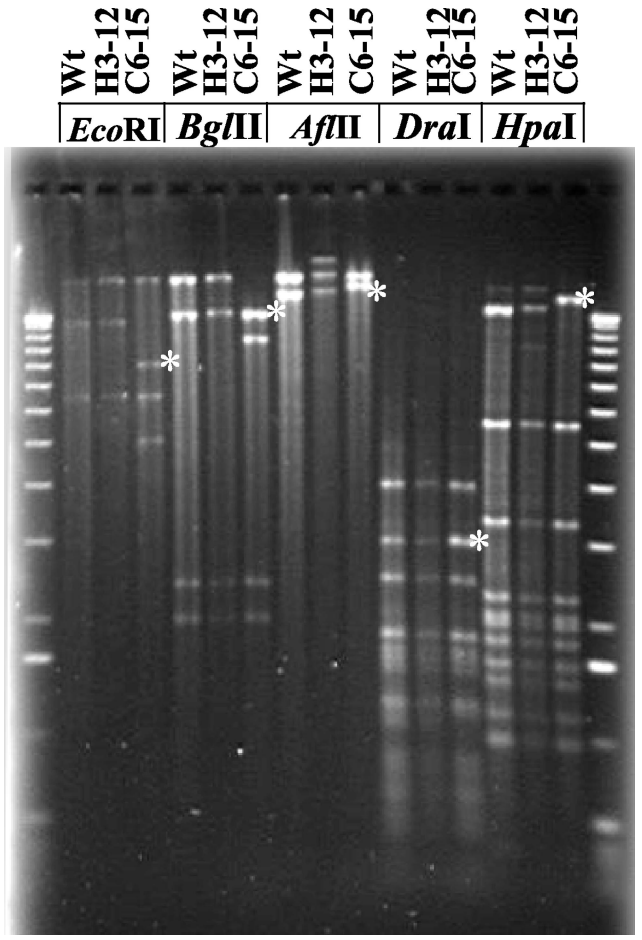

FIG. 4. Restriction digestion of wild-type, H3-12, and C6-15/*parE* plasmids with EcoRI, BglII, AflII, DraI, and HpaI. The gel was used for Southern blot analysis by probing with mini-Tn*5*. Bands hybridizing to the Tn*5* probe (asterisks) were identified. Wt, wild type.

of the urinary tract. Homologs were identified in other species for 29 sequences. Twenty-five of the mutants were out-competed by the wild-type strain by more than a 100-fold in the murine urinary tract. Three of the mutations (in mutants B6-40, E5-36, and F4-37) eliminated the activity or diminished the synthesis of three previously identified virulence factors (urease, flagella, and MR/P fimbriae, respectively). Other mutants identified a requirement for chemotaxis (E6-43) and phosphate transport (G1-43 and H4-34) for virulence of *P. mirabilis* in the urinary tract. In addition, two attenuated mutants (C4-41 and C6-15) were identified with transposon insertions in a ~42-kb plasmid of *P. mirabilis* HI4320 (Fig. 1B), raising the possibility that there is a virulence plasmid in this strain. It is instructive to discuss, in the context of previously published reports, possible explanations for attenuation of mutants with transposon insertions in *ureF*, *cheW*, *dsbA*, two-component sensor kinase and phosphate transport genes, iron acquisition genes, and plasmid stability genes, as well as genes encoding metabolic functions. The findings further support the ability of this technique to identify genes based simply on the in vivo survival phenotype or a lack thereof.

Established virulence factors. Synthesis of three known virulence factors (11, 55, 59), urease, flagella, and MR/P fimbriae, was eliminated or diminished by three independent mutations. Identification of known virulence-associated genes verified that STM can be used successfully to identify virulence factors in uropathogenic *P. mirabilis* with the CBA mouse model of infection. The urease-negative mutant B6-40 had a transposon insertion in the *ureF* gene. This mutant was completely outcompeted by wild-type strain HI4320 within the detection limits of the CBA mouse model in the bladder and kidneys. The urease gene cluster includes three structural genes, *ureA*, *ureB*, and *ureC*, in addition to four accessory genes, *ureD*, *ureE*, *ureF*, *and ureG*. The urease apoenzyme is comprised of a trimeric complex of the trimer UreABC (that is, three copies of each subunit) (36). Activation of this urease apoenzyme requires incorporation of nickel ions into the metallocenter located in UreC (64). The accessory proteins UreD, UreE, UreF, and UreG coordinate activation of the functional urease enzyme by mediating incorporation of the nickel ions into the active site (58). Mutation of any of these four accessory genes results in synthesis of an inactive apoenzyme (35). The B6-40 mutant was urease negative but produced the UreC subunit. Synthesis of the UreC subunit was expected, since the effect of mutation of *ureF*, which is downstream of *ureC*, should be confined to nickel incorporation into the apoenzyme.

The mutated gene in a second attenuated mutant, E6-43, is homologous to *cheW*, a component of the chemotaxis regulatory system. Chemotaxis mediates bacterial movement toward attractants and away from repellants by using proteins that transmit signals from the transmembrane receptor proteins (methyl-accepting chemotaxis proteins [MCPs]) to the flagellar motor. These chemoreceptors function as ternary complexes composed of CheA, CheW, and MCP, where CheA autophosphorylates in response to repellant stimuli bound to MCP. Phosphorylated CheA donates the phosphoryl group to CheY, which diffuses to the flagellar motor and initiates clockwise rotation, mediating tumbling. In vitro research has suggested that CheW functions as an adaptor protein coupling CheA to MCP (27, 76, 77). Boukhvalova et al. (9) showed that *E. coli cheW* mutants, with disrupted CheW binding sites for the Tar receptor or CheA, lacked active ternary complexes in vitro and chemotaxis capabilities in vivo. Phenotypic analysis of the E6-43 mutant showed that swarming activity was severely compromised compared to that of wild-type strain HI4320 (Fig. 2), indicating that disruption of *cheW* influences the swimmer-swarmer differentiation observed on plates in vitro. Attenuation in the mouse model suggests that the chemotactic response is vital to *P. mirabilis* movement and colonization within the host.

A third mutant, mutant F4-37, had a transposition in a gene encoding a protein that was nearly identical to DsbA, a periplasmic protein that catalyzes disulfide bond formation within periplasmic, outer membrane, and secreted proteins. The F4-37 mutant was completely out-competed by the parental HI4320 strain in the cochallenge experiments, and the mutant displayed an altered swarming phenotype compared to the phenotype of the parental *P. mirabilis* strain. DsbA mutations have been implicated in deficiencies in motility, fimbriation, and protein secretion. In uropathogenic *E. coli*, DsbA is required for protein folding of the PapD chaperone and adhesive

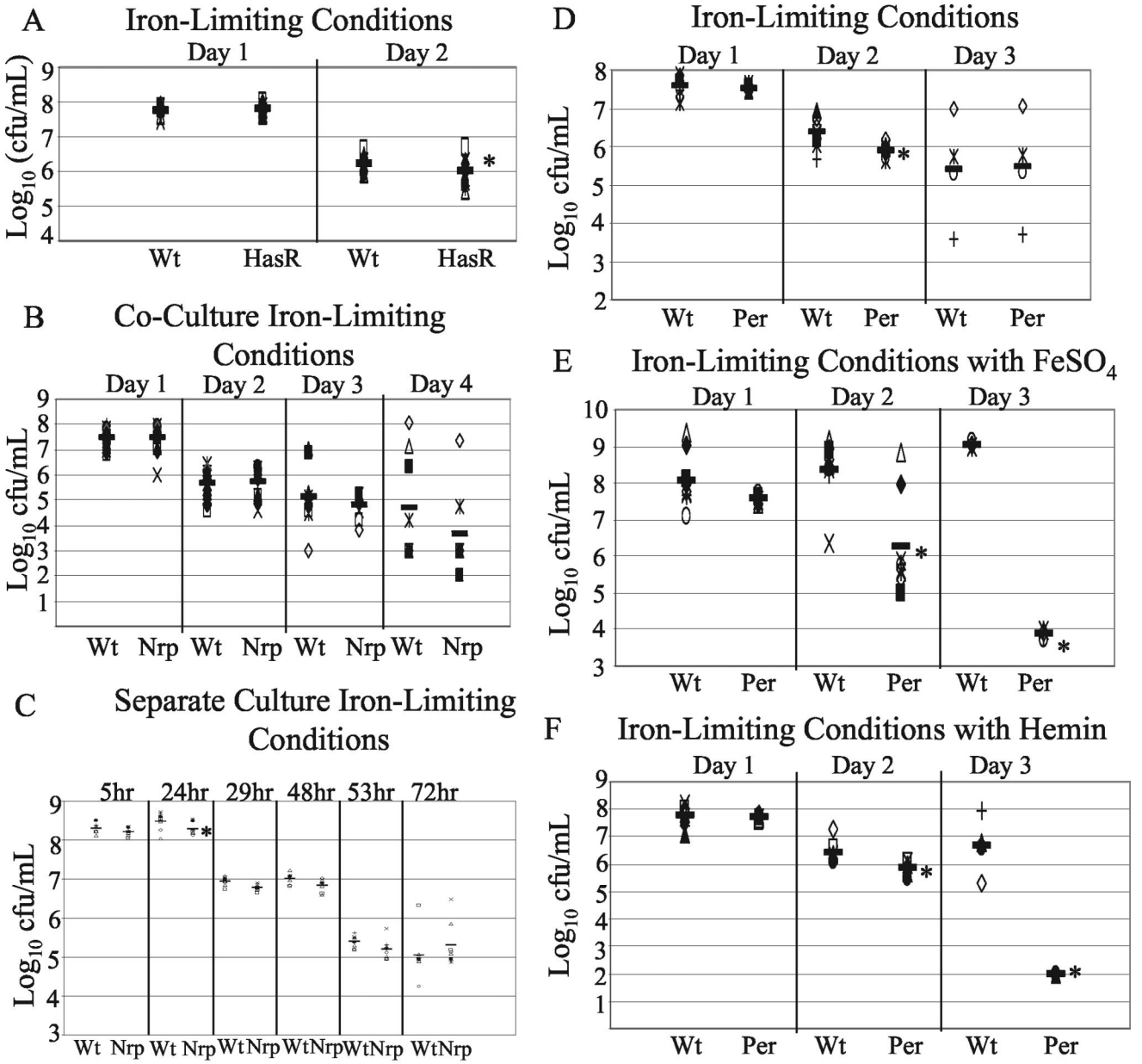

FIG. 5. Iron-limited growth studies of *P. mirabilis* signature-tagged mutants G4-2, A1-8, and H3-12. In vitro cocultures of the *P. mirabilis* wild type with G4-2/HasR (A), A1-8/NrpG (B), and H3-12/iron transport permease (D) were grown in iron-limited rich medium, and separate cultures of the *P. mirabilis* wild type and A1-8/NrpG (C) were grown in iron-limited rich medium. Cocultures of the *P. mirabilis* wild type with H3-12/iron transport permease were grown in iron-limited rich medium supplemented with $FeSO_4$ (E) and hemin (F). Each distinct symbol for the coculture experiments corresponds to a distinct tube with the wild-type and mutant counts paired. Each distinct symbol for the separate culture experiment corresponds to bacterial counts in two randomly paired tubes, one containing only the wild type and one containing only A1-8. Tubes were not paired for statistical analysis. The solid bars indicate geometric means. An asterisk indicates mutant counts that were statistically significantly different from the wild-type counts. Wt, wild type; Per, iron transport permease.

P pilus assembly (37), and it was identified in an STM screening in uropathogenic *E. coli* CFT073 in the urinary tract (4). Other pathogenic gram-negative species with mutations in *dsbA* are deficient in bundle-forming pili (18), heat-labile enterotoxin (92), F pili (5), cholera toxin, and Tcp pili (65). Mutation of DsbA also inhibits disulfide bond formation in OmpA, β-lactamase, and alkaline phosphatase (5, 44) and can affect motility (5, 16). Interestingly, Western analysis indicated that the F4-37 mutant produced flagellin protein (faintly) and was capable of swarming (albeit aberrantly), but it lacked detectable levels of the MR/P or ambient temperature fimbria components. Since *dsbA* defects alter many outer membrane, fimbrial, and secreted proteins, it is likely that additional virulence factors are disrupted in mutant F4-37 and act synergistically to ablate colonization in the CBA mouse model.

Iron acquisition. Microorganisms, specifically pathogens, possess a variety of iron acquisition mechanisms to overcome low free iron concentrations encountered in the host, which

tend to be 10^8-fold lower than the concentration necessary for growth (89). Mechanisms of iron acquisition include (i) direct utilization of the host iron compounds, including heme, hemoglobin, transferrin, and lactoferrin and (ii) synthesis of high-affinity iron-chelating molecules, known as siderophores, that are secreted into the iron-limiting environment to scavenge extracellular iron (14). Four mutants were identified as having iron acquisition gene homologs, including *nrpG*, *hasR*, and genes encoding an iron transport permease and an iron-regulated outer membrane protein. A previous study revealed that the upstream region of the *P. mirabilis nrp* operon contains a putative Fur box overlapping the −35 region of the promoter and that the operon is iron regulated (26). Based on the high level of homology of *nrp* genes to the yersiniabactin system and on the fact that the *nrp* operon is iron regulated, the possibility was raised that *P. mirabilis* produces a siderophore that has not been detected previously. In a separate study, Evanylo et al. (23) proposed that an α-keto acid produced by a deaminase activity in *P. mirabilis* was involved in iron chelation. Attempts in our lab to determine whether *P. mirabilis* uses this α-keto acid as an iron chelator also pointed us toward a deaminase (51). However, the cloned *aad* (amino acid deaminase) gene was unable restore iron-limiting survival in a siderophore-negative *E. coli* strain, which was also unable to use exogenously provided α-keto acid; thus, no role for this deaminase in iron acquisition could be verified or ruled out. Finally, CAS agar tests were not able to identify an iron-chelating activity associated with *P. mirabilis* (51).

The *nrp* operon encodes a nonribosomal polypeptide-polyketide synthesis system, which is used by bacteria to make a variety of small compounds, including antibacterial compounds, toxins, and siderophores (26). The *nrpG* gene encodes a phosphopantetheinyl transferase, and inactivation of this gene results in loss of the required modification of the carrier domains for nonribosomal polypeptide and polyketide synthases (45, 84). The 4′-phosphopantetheine attachment serves as an arm for attaching the growing product and transferring it to other domains in the synthase (10, 45, 85). The final secreted product appears to be complemented in an in vitro coculture since coculture restores the attenuation seen briefly in separate cultures in which bacteria are more likely to come into close contact than in the urinary tract, where colonizing bacteria may be more diffusely located. Growth of the *nrpG* mutant tended to be reduced in iron-limiting conditions compared to wild-type growth (Fig. 5). The failure of another strain to complement the secreted product in vivo may suggest that the product has a limited half-life or diffusion range, potentially due to urea or other environmental conditions, which, coupled with the more diffuse localization of bacteria, could prevent complementation within the urinary tract of the mouse.

The HasR homolog appears to play a minor role in iron acquisition based on the minimal reduction in survival in iron-limiting conditions and the recovery of the mutant by supplementation with hemin or $FeSO_4$ (Fig. 5). This mirrors the attenuation of this mutant seen in the kidneys, where heme would likely be a dominant iron source, and it suggests that there are other homologs in the genome that are more critical. Additionally, other studies have suggested that membrane-bound heme receptors are not the most sensitive means for heme acquisition, as many bacteria have evolved a secreted hemophore that transports the heme to a membrane receptor, greatly enhancing heme uptake (28, 47). Thus, this system of heme uptake may lack the affinity necessary to make it a critical system for survival under iron-limiting conditions.

The iron transport permease appears to play a role in survival in iron-limiting conditions, and an iron transport permease mutant is handicapped compared to the wild-type when there is an external source of iron (Fig. 5). The latter information suggests that the ability to use this permease for uptake is preferred and that its loss is not complemented by other systems when alternate iron sources are provided. Additionally, these results support the hypothesis that there is some form of secreted siderophore. While it has been shown that some bacteria express permeases capable of transporting siderophores of other strains (82), the infection model which we used did not produce mixed populations of bacteria that might produce a siderophore since the urinary tract was sterile until the infecting bacterium was introduced.

Mutant D6-33, the most attenuated mutant, has a disruption in a gene with significant homology to genes encoding a putative outer membrane protein in *Yersinia* sp. and IrgA, an iron-regulated virulence protein in *V. cholerae*. This homology suggests that the mutation knocked out a siderophore receptor gene. This mutant was out-competed >10,000-fold in the bladder, and its level tended to be reduced in the kidney compared to the level of the parental strain (Table 1). Recent work has demonstrated that *V. cholerae* possesses two separate enterobactin receptors, IrgA and VctA, for the acquisition of exogenous enterobactin sources (54). Additionally, Mey et al. showed that the *irgA* mutant retains the ability to colonize the infant mouse model of *V. cholerae* virulence at levels equivalent to those of the wild-type parental strain. Perhaps these results are not unexpected since the *irgA* mutant retains the ability to utilize exogenous enterobactin sources via the alternative VctA transport mechanism. Members of genera in the family *Enterobacteriaceae*, including *Escherichia*, *Salmonella*, *Klebsiella*, and *Shigella*, have the genes encoding the catecholate siderophore enterobactin (14).

Transcriptional regulators. A third group of interesting mutants encoding DNA binding proteins revealed virulence regulators that merit further study. The gene encoding the LysR/HdfR homolog was hit independently twice, once in sequences encoding the N-terminal DNA binding region and once in the region encoding the C-terminal substrate binding domain. Since this group of regulators is implicated in regulation of the master flagellar operon genes, *flhDC*, one would predict that the attenuation of these mutants may be linked to their motility. Both of the mutants, however, have a normal swarming phenotype on an agar surface. Nevertheless, the LysR/HdfR homolog may provide new clues regarding the regulation of genes essential for colonization and spread within the UTI.

The attenuated mutant E5-36 has a disruption in a gene encoding a two-component system sensor kinase protein. Environmental signals evoke bacterial responses through transmembrane signal transduction systems composed of a sensor kinase that autophosphorylates on a histidine residue and a response regulator that accepts the phosphoryl group from the sensor kinase (63). Interestingly, mutant E5-36 is deficient for swarming on an agar surface, and Western analysis revealed a diminished level of the flagellar structural subunit, flagellin

(Fig. 2G). The deficiency of this two-component system likely gives wild-type *P. mirabilis* strain HI4320 an advantage over mutant E5-36 during murine cochallenge experiments, since E5-36 cannot initiate the proper signaling response to the environmental stimuli (note that this mutant was also eliminated during in vitro STM in minimal medium). The specific environmental stimulus that initiates signaling through this sensor kinase is unknown, while the in vitro swarming deficiency and the deficiency of the flagellin component allow us to speculate that the signaling pathway regulates differentiation and flagellar expression. Allison et al. (1) demonstrated that *P. mirabilis* mutants with swarming-deficient or nonswarming phenotypes were unable to colonize the kidneys in a mouse model of ascending UTI, while only the nonswarming mutants failed to colonize the bladder.

Plasmid function. The results obtained for two mutants, the *parE* and *pilX3* mutants, supported a role in virulence for the large (~42-kb) plasmid of *P. mirabilis* HI4320. The mutation in the C6-15 transposon insertion mutant, one of the most attenuated mutants identified, is in a *parE* homolog, which encodes the toxin component of a toxin-antitoxin plasmid maintenance system, *parDE* (19, 41). However, this operon is always coupled with another operon, *parABC*, which encodes a resolvase, ParA, involved in plasmid maintenance. Both operons appear to be required for the full stabilization observed in plasmids with this maintenance system (19, 41). While not all strains of *P. mirabilis* contain a plasmid, this strain was attenuated in vivo. A possible genetic basis for its attenuation may be the instability of its large plasmid, which has substantial changes in its restriction profile, independent of the insertion event (Fig. 2). Evidence that this plasmid is important in virulence comes from preliminary sequencing data suggesting that an *nrp* gene homolog, which is missing in the *nrp* operon, is carried on the plasmid in strain HI4320 (15, 26; A. Merla, J. Dattelbaum, and H. Mobley; unpublished data). Thus, complete function of the *nrp* operon could require a plasmid-borne gene.

Mutant C4-41 has a disrupted gene that has limited homology to the *E. coli* gene encoding protein PilX3, an outer membrane protein that is likely part of the conjugative pilus structure. The *pilX3* gene is encoded on the large (~42-kb) plasmid in the *P. mirabilis* HI4320 strain (Fig. 3B). Identification of mutant C4-41 as a *pilX3* mutant is tentative due to the limited DNA sequence available for analysis. Nevertheless, attenuation due to transposon insertion within the plasmid suggests that the plasmid is necessary for full virulence.

Capsule. Two *P. mirabilis* mutants, D6-26 and G5-30, were completely out-competed by wild-type strain HI4320 in cochallenge experiments, and both of these mutants have swarming deficiencies in vitro (Fig. 2C and D). Sequence analysis revealed that the D6-26 mutated gene encodes a protein that is homologous to a putative glycosylase (*Y. pestis*) and has conserved domain features similar to those of LppC, a putative lipoprotein. Analysis of the G5-30 mutant revealed that the mutated gene encodes a protein that is homologous to hypothetical proteins from *Y. pestis* and *E. coli* and has conserved domain features similar to those of a predicted xylanase and polysaccharide deacetylase. These domain characterizations suggest a possible role in alteration in the extracellular capsule structure, which is crucial for swarming and a vital factor in *Proteus* infection.

Metabolic and synthetic genes. The identification of mutations in nine metabolic genes that do not appear to affect survival in minimal A medium suggests that these genes may play a role in virulence beyond their putative metabolic functions and suggests that specific nutrients may be limiting in the urinary tract. The carbamoyl phosphate synthetase, for example, produces carbamoyl phosphate, which is used to synthesize certain purines and as an intermediate to urea in the urea cycle. The inability to make purines probably prevents this mutant from growing in minimal medium, as well as in the urinary tract. The HemY homolog, which catalyzes a late step in protoheme IX synthesis, could affect the ability of the mutant to produce heme for use as a prosthetic group in cytochromes and catalases, possibly reducing the growth rate in minimal medium and, thus, competitive survival. Interestingly, the phosphoserine aminotransferase mutant (G4-12) was recovered from the minimal medium STM screening, and growth studies showed that there was no reduction in the growth rate compared to the growth rate of the wild type (Table 2 and data not shown). The mutation event involved insertion of the transposon 47 bp upstream of the translational start site, separating the ORF from its putative promoter. The transposon contains a transcriptional terminator, which should prevent any read-through from an upstream promoter. An additional function, inhibition of septation, has been linked to mutation of this gene independent of its serine and pyrodoxine biosynthetic abilities (61).

We isolated two mutants, H4-34 and G1-43, with insertions in separate genes, *pstS* and *pstC*, within the operon encoding an inorganic phosphate transport system. *E. coli* maintains two transport systems for inorganic phosphate acquisition: the phosphate-specific transport system (Pst system) and the P_i transport system (Pit system) (75). Under normal growth conditions, *E. coli* constitutively expresses the single transport protein, Pit, which has a low affinity for inorganic phosphate. In limiting conditions for inorganic phosphate, inorganic phosphate acquisition is mediated by the Pst system, which is comprised of PstS, PstC, PstA, and PstB (71). The Pst system acts as an ABC transporter across the inner membrane, in which PstC and PstA are integral membrane proteins that mediate P_i translocation from the periplasmic binding protein, PstS, to the cytosol (88). Under P_i-limiting conditions, assimilation of inorganic phosphate by *E.coli* is eliminated by single mutations of the following genes: *pstS*, *pstC*, *pstA*, and *pstB* (13, 78, 91). An inability to acquire phosphate under nutrient-limiting conditions in vivo in itself would explain attenuation; additional effects on *pho*-regulated gene expression (86) may also occur and explain the low fitness of these mutants.

Mutant E6-41 has a disruption in the gene that encodes the regulatory protein AsnC and was out-competed 100-fold by parental strain HI4320 in the bladder and kidneys upon cochallenge in the CBA mouse model. The *E. coli* genome contains two asparagine synthetase genes, *asnA* and *asnB*, whose products convert aspartate into asparagine. The AsnA synthetase utilizes ammonium as a nitrogen donor, whereas the AsnB synthetase can mediate donation of an amino group from glutamine or ammonium to the aspartate residue. AsnC is the positive activator of the AsnA synthetase, and the AsnC-dependent activation of *asnA* is suppressed by asparagine through an unknown mechanism (46). Under nitrogen-excess

conditions, *E. coli* synthesizes asparagine by utilization of the ammonium by AsnA and AsnB (74). Under nitrogen-limiting conditions, the *E. coli* AsnB synthesizes asparagine from cellular glutamine produced by glutamine synthetase conversion of ammonium, whereas AsnA activity is eliminated by repression of its transcriptional activator, *asnC*, by the protein Nac (nitrogen assimilation control protein) of the Ntr system (69). *P. mirabilis* mutant E6-41 exhibited reduced growth on minimal A medium, which indicates that *P. mirabilis* likely has a second asparagine synthetase that maintains the viability of the mutant in vitro. The finding that mutant E6-41 was out-competed by wild-type strain HI4320 in retrospect may have been expected, because of the nature of the *P. mirabilis* infection and the overproduction of ammonia from urease-mediated urease hydrolysis. The excess nitrogen in vivo promotes ammonium utilization by the AsnA and AsnB synthetases; therefore, the limited AsnB activity of mutant E6-41 may account for the reduced infectivity in the CBA murine model.

Mutant G1-38 was identified as an attenuated mutant from cochallenge data, but it exhibited normal growth on minimal salts medium. The interrupted gene is homologous to the 3-deoxy-D-arabinoheptulosonate-7-phosphate (DAHP) synthase that is phenylalanine repressible and is encoded by *aroG*. The initial step in the biosynthesis of aromatic amino acids and vitamins is catalyzed by the DAHP synthase. The *E. coli* genome has genes for three DAHP synthase isoenzymes, AroF, AroG, and AroH, which are sensitive to the levels of the amino acids tyrosine, phenylalanine, and tryphophan, respectively (68). In *E. coli*, each DAHP synthase isoenzyme contributes to the total DAHP synthase activity. Analysis of the composition of the total DAHP synthase activity has shown that Phe-, Tyr-, and Trp-sensitive DAHP synthases contribute 80, 20, and 1% of the total activity, respectively (83). Surprisingly, the *aroG* mutant exhibited normal growth on minimal salts medium; therefore, the *aroF* and *aroH* genes must augment mutant growth in vitro. While these mutants retain sufficient protein levels for in vitro survival, the mutants are clearly not as fit as the wild-type strain and are out-competed by it in the host.

One attenuated mutant, F1-29, had a Tn*5* insertion in a gene with homology to *yhdG*, a putative dihydrouridine synthase gene. 5,6-Dihydrouridine is a modified base found in the D loops of tRNA from archaea, bacteria, and eukarya (79). Most *E. coli* tRNAs contain one or more dihydrouridine residues, and only $tRNA^{Tyr}$ and $tRNA^{Glu}$ have no dihydrouridine residues (8). The dihydrouridine residues localized within the tRNA were shown to destabilize the structure and are thought to confer conformational flexibility to the tRNA molecules (17). One can speculate that the effects of reduced tRNA stability could be exacerbated during infection due to the increased protein synthesis requirements (53), and this may explain the normal growth observed in vitro.

Mutant D6-39 was out-competed by *P. mirabilis* HI4320 in both the bladder and kidneys, and its disrupted gene encodes a homolog of NrdD, the anaerobic ribonucleotide reductase. Ribonucleotide reductase produces the deoxyribonucleotide triphosphate by ribonucleotide reduction, for DNA replication. *E. coli* synthesizes two distinct ribonucleotide reductases, one for aerobic conditions and one for anaerobic conditions (72). The *E. coli* aerobic reductase is a class I enzyme and requires oxygen to function (21, 25, 73). The *E. coli* anaerobic reductase is a class III reductase containing an iron-sulfur center and a glycyl radical (62, 81), and its activity is limited to anaerobic conditions due to stability under anaerobic growth conditions and destruction of the glycyl radical by oxygen, which renders the enzyme nonfunctional during aerobic growth (81). Research in our lab has suggested that during infection and colonization of the bladder, *P. mirabilis* experiences oxygen-limiting conditions, especially when the number of CFU is high (Li and Mobley, submitted for publication). If mutant D6-39 lacks the anaerobic ribonucleotide reductase and the aerobic enzyme is oxygen dependent, the mutant would be deficient in deoxyribonucleoside triphosphates for DNA synthesis under the oxygen-limiting conditions faced in the bladder at a high bacterial density.

Taken together, these findings suggest that when the functions of metabolic genes are assessed, survival should be quantified both under nutrient limitation conditions in vitro and in an animal model to establish whether the actual roles are metabolic or are associated with virulence.

Colocalizing homologs. Two mutants, A3-39 and F6-34, were attenuated for colonization of the bladder and kidneys compared to parental strain HI4320, and the mutant proteins have significant homology to the YtfM and YtfN putative proteins, respectively, encoded by adjacent genes within the *msrA-chpB* intergenic region of the *E. coli* CFT073 genome (positions 5058279 to 5060012) (90). The functions of YtfN and YftM remain unknown; however, a YtfN homolog was also identified as attenuated in the bladders of mice in an STM study of *Klebsiella pneumoniae* (80).

Summary. A rigorous four-step screening procedure was used to identify 25 highly attenuated (>100-fold) mutants, which represented 1.2% of more that 2,000 mutants tested. Most of these mutants do not have obvious phenotypes, and it would have been difficult to identify the mutant genes as virulence determinants by conventional methods. While enumeration of such virulence genes is critical, complete biological evaluation of these mutants, including complementation, is necessary to fully understand the role of the genes in the pathogenesis of UTI caused by *P. mirabilis* and to satisfy molecular Koch's postulates as formulated by Falkow (24).

ACKNOWLEDGMENTS

We thank Chris Tang for the gift of signature-tagged transposon plasmids.

This work was supported in part by Public Health Service grant DK49720 from the National Institutes of Health.

REFERENCES

1. **Allison, C., L. Emody, N. Coleman, and C. Hughes.** 1994. The role of swarm cell differentiation and multicellular migration in the uropathogenicity of *Proteus mirabilis*. J Infect. Dis. **169:**1155–1158.
2. **Ausubel, F. M., R. Brent, R. E. Kingston, D. D. Moore, J. G. Seidman, J. A. Smith, and K. Struhl (ed.).** 1995. Current protocols in molecular biology, p. 10.8.1–10.8.17. John Wiley & Sons, Inc., New York, N.Y.
3. **Bacheller, C. D., and J. M. Bernstein.** 1997. Urinary tract infections. Med. Clin. N. Am. **81:**719–730.
4. **Bahrani-Mougeot, F. K., E. L. Buckles, C. V. Lockatell, J. R. Hebel, D. E. Johnson, C. M. Tang, and M. S. Donnenberg.** 2002. Type 1 fimbriae and extracellular polysaccharides are preeminent uropathogenic *Escherichia coli* virulence determinants in the murine urinary tract. Mol. Microbiol. **45:**1079–1093.
5. **Bardwell, J. C., K. McGovern, and J. Beckwith.** 1991. Identification of a protein required for disulfide bond formation in vivo. Cell **67:**581–589.
6. **Belas, R.** 1996. *Proteus mirabilis* swarmer cell differentiation and urinary tract infection, p. 271–298. *In* J. W. Warren (ed.), Urinary tract infections: mo-

lecular pathogenesis and clinical management. ASM Press, Washington, D.C.
7. **Belas, R., D. Erskine, and D. Flaherty.** 1991. Transposon mutagenesis in *Proteus mirabilis*. J. Bacteriol. **173:**6289–6293.
8. **Bishop, A. C., J. Xu, R. C. Johnson, P. Schimmel, and V. de Crecy-Lagard.** 2002. Identification of the tRNA-dihydrouridine synthase family. J. Biol. Chem. **277:**25090–25095.
9. **Boukhvalova, M. S., F. W. Dahlquist, and R. C. Stewart.** 2002. CheW binding interactions with CheA and Tar. Importance for chemotaxis signaling in *Escherichia coli*. J. Biol. Chem. **277:**22251–22259.
10. **Cane, D. E., and C. T. Walsh.** 1999. The parallel and convergent universes of polyketide synthases and nonribosomal peptide synthetases. Chem. Biol. **6:**R319–R325.
11. **Coker, C., C. A. Poore, X. Li, and H. L. T. Mobley.** 2000. Pathogenesis of *Proteus mirabilis* urinary tract infection. Microbes Infect. **2:**1497–1505.
12. **Coudron, P. E., E. S. Moland, and K. S. Thomson.** 2000. Occurrence and detection of AmpC beta-lactamases among *Escherichia coli*, *Klebsiella pneumoniae*, and *Proteus mirabilis* isolates at a veterans medical center. J. Clin. Microbiol. **38:**1791–1796.
13. **Cox, G. B., H. Rosenberg, J. A. Downie, and S. Silver.** 1981. Genetic analysis of mutants affected in the Pst inorganic phosphate transport system. J. Bacteriol. **148:**1–9.
14. **Crosa, J. H.** 1989. Genetics and molecular biology of siderophore-mediated iron transport in bacteria. Microbiol. Rev. **53:**517–530.
15. **Crosa, J. H., and C. T. Walsh.** 2002. Genetics and assembly line enzymology of siderophore biosynthesis in bacteria. Microbiol. Mol. Biol. Rev. **66:**223–249.
16. **Dailey, F. E., and H. C. Berg.** 1993. Mutants in disulfide bond formation that disrupt flagellar assembly in *Escherichia coli*. Proc. Natl. Acad. Sci. **90:**1043–1047.
17. **Dalluge, J. J., T. Hashizume, A. E. Sopchik, J. A. McCloskey, and D. R. Davis.** 1996. Conformational flexibility in RNA: the role of dihydrouridine. Nucleic Acids Res. **24:**1073–1079.
18. **Donnenberg, M. S., H. Z. Zhang, and K. D. Stone.** 1997. Biogenesis of the bundle-forming pilus of enteropathogenic *Escherichia coli*: reconstitution of fimbriae in recombinant *E.coli* and role of DsbA in pilin stability—a review. Gene **192:**33–38.
19. **Easter, C. L., P. A. Sobecky, and D. R. Helinski.** 1997. Contribution of different segments of the *par* region to stable maintenance of the broad-host-range plasmid RK2. J. Bacteriol. **179:**6472–6479.
20. **Edelstein, P. H., M. A. Edelstein, F. Higa, and S. Falkow.** 1999. Discovery of virulence genes of *Legionella pneumophila* by using signature-tagged mutagenesis in a guinea pig pneumonia model. Proc. Natl. Acad. Sci. **96:**8190–8195.
21. **Eliasson, R., E. Pontis, M. Fontecave, C. Gerez, J. Harder, H. Jornvall, M. Krook, and P. Reichard.** 1992. Characterization of components of the anaerobic ribonucleotide reductase system from *Escherichia coli*. J. Biol. Chem. **267:**25541–25547.
22. **Esposito, A. L., R. A. Gleckman, S. Cram, M. Crowley, F. McCabe, and M. S. Drapkin.** 1980. Community-acquired bacteremia in the elderly: analysis of one hundred consecutive episodes. J. Am. Geriatr. Soc. **28:**315–319.
23. **Evanylo, L. P., S. Kadis, and J. R. Maudsley.** 1984. Siderophore production by *Proteus mirabilis*. Can. J. Microbiol. **30:**1046–1051.
24. **Falkow, S.** 1988. Molecular Koch's postulates applied to microbial pathogenicity. Rev. Infect. Dis. **10**(Suppl. 2)**:**S274–S276.
25. **Fontecave, M., P. Nordlund, H. Eklund, and P. Reichard.** 1992. The redox centers of ribonucleotide reductase of *Escherichia coli*. Adv. Enzymol. Relat. Areas Mol. Biol. **65:**147–183.
26. **Gaisser, S., and C. Hughes.** 1997. A locus coding for putative non-ribosomal peptide/polyketide synthase functions is mutated in a swarming-defective *Proteus mirabilis* strain. Mol. Gen. Genet. **253:**415–427.
27. **Gegner, J. A., D. R. Graham, A. F. Roth, and F. W. Dahlquist.** 1992. Assembly of an MCP receptor, CheW, and kinase CheA complex in the bacterial chemotaxis signal transduction pathway. Cell **70:**975–982.
28. **Ghigo, J. M., S. Letoffe, and C. Wandersman.** 1997. A new type of hemophore-dependent heme acquisition system of *Serratia marcescens* reconstituted in *Escherichia coli*. J. Bacteriol. **179:**3572–3579.
29. **Griffith, D. P.** 1978. Struvite stones. Kidney Int. **13:**372–382.
30. **Griffith, D. P.** 1979. Urease stones. Urol. Res. **7:**215–221.
31. **Hagberg, L., I. Engberg, R. Freter, J. Lam, S. Olling, and C. Svanborg Eden.** 1983. Ascending, unobstructed urinary tract infection in mice caused by pyelonephritogenic *Escherichia coli* of human origin. Infect. Immun. **40:**273–283.
32. **Heimer, S. R., and H. L. Mobley.** 2001. Interaction of *Proteus mirabilis* urease apoenzyme and accessory proteins identified with yeast two-hybrid technology. J. Bacteriol. **183:**1423–1433.
33. **Hensel, M., J. E. Shea, C. Gleeson, M. D. Jones, E. Dalton, and D. W. Holden.** 1995. Simultaneous identification of bacterial virulence genes by negative selection. Science **269:**400–403.
34. **Hu, L. T., E. B. Nicholson, B. D. Jones, M. J. Lynch, and H. L. Mobley.** 1990. *Morganella morganii* urease: purification, characterization, and isolation of gene sequences. J. Bacteriol. **172:**3073–3080.
35. **Island, M. D., and H. L. Mobley.** 1995. *Proteus mirabilis* urease: operon fusion and linker insertion analysis of *ure* gene organization, regulation, and function. J. Bacteriol. **177:**5653–5660.
36. **Jabri, E., M. B. Carr, R. P. Hausinger, and P. A. Karplus.** 1995. The crystal structure of urease from *Klebsiella aerogenes*. Science **268:**998–1004.
37. **Jacob-Dubuisson, F., J. Pinkner, Z. Xu, R. Striker, A. Padmanhaban, and S. J. Hultgren.** 1994. PapD chaperone function in pilus biogenesis depends on oxidant and chaperone-like activities of DsbA. Proc. Natl. Acad. Sci **91:**11552–11556.
38. **Jansen, A. M., C. V. Lockatell, D. E. Johnson, and H. L. Mobley.** 2003. Visualization of *Proteus mirabilis* morphotypes in the urinary tract: the elongated swarmer cell is rarely observed in ascending urinary tract infection. Infect. Immun. **71:**3607–3613.
39. **Johnson, D. E., C. V. Lockatell, M. Hall-Craigs, H. L. Mobley, and J. W. Warren.** 1987. Uropathogenicity in rats and mice of *Providencia stuartii* from long-term catheterized patients. J. Urol. **138:**632–635.
40. **Johnson, D. E., R. G. Russell, C. V. Lockatell, J. C. Zulty, J. W. Warren, and H. L. Mobley.** 1993. Contribution of *Proteus mirabilis* urease to persistence, urolithiasis, and acute pyelonephritis in a mouse model of ascending urinary tract infection. Infect. Immun. **61:**2748–2754.
41. **Johnson, E. P., A. R. Strom, and D. R. Helinski.** 1996. Plasmid RK2 toxin protein ParE: purification and interaction with the ParD antitoxin protein. J. Bacteriol. **178:**1420–1429.
42. **Jones, B. D., C. V. Lockatell, D. E. Johnson, J. W. Warren, and H. L. Mobley.** 1990. Construction of a urease-negative mutant of *Proteus mirabilis*: analysis of virulence in a mouse model of ascending urinary tract infection. Infect. Immun. **58:**1120–1123.
43. **Jones, B. D., and H. L. Mobley.** 1989. *Proteus mirabilis* urease: nucleotide sequence determination and comparison with jack bean urease. J. Bacteriol. **171:**6414–6422.
44. **Kamitani, S., Y. Akiyama, and K. Ito.** 1992. Identification and characterization of an *Escherichia coli* gene required for the formation of correctly folded alkaline phosphatase, a periplasmic enzyme. EMBO J. **11:**57–62.
45. **Keating, T. A., and C. T. Walsh.** 1999. Initiation, elongation, and termination strategies in polyketide and polypeptide antibiotic biosynthesis. Curr. Opin. Chem. Biol. **3:**598–606.
46. **Kolling, R., and H. Lother.** 1985. AsnC: an autogenously regulated activator of asparagine synthetase A transcription in *Escherichia coli*. J. Bacteriol. **164:**310–315.
47. **Letoffe, S., C. Deniau, N. Wolff, E. Dassa, P. Delepelaire, A. Lecroisey, and C. Wandersman.** 2001. Haemophore-mediated bacterial haem transport: evidence for a common or overlapping site for haem-free and haem-loaded haemophore on its specific outer membrane receptor. Mol. Microbiol. **41:**439–450.
48. **Li, X., D. E. Johnson, and H. L. Mobley.** 1999. Requirement of MrpH for mannose-resistant *Proteus*-like fimbria-mediated hemagglutination by *Proteus mirabilis*. Infect. Immun. **67:**2822–2833.
49. **Li, X., H. Zhao, C. V. Lockatell, C. B. Drachenberg, D. E. Johnson, and H. L. Mobley.** 2002. Visualization of *Proteus mirabilis* within the matrix of urease-induced bladder stones during experimental urinary tract infection. Infect. Immun. **70:**389–394.
50. **Maroncle, N., D. Balestrino, C. Rich, and C. Forestier.** 2002. Identification of *Klebsiella pneumoniae* genes involved in intestinal colonization and adhesion using signature-tagged mutagenesis. Infect. Immun. **70:**4729–4734.
51. **Massad, G., H. Zhao, and H. L. Mobley.** 1995. *Proteus mirabilis* amino acid deaminase: cloning, nucleotide sequence, and characterization of *aad*. J. Bacteriol. **177:**5878–5883.
52. **Mei, J. M., F. Nourbakhsh, C. W. Ford, and D. W. Holden.** 1997. Identification of *Staphylococcus aureus* virulence genes in a murine model of bacteraemia using signature-tagged mutagenesis. Mol. Microbiol. **26:**399–407.
53. **Merrell, D. S., S. M. Butler, F. Qadri, N. A. Dolganov, A. Alam, M. B. Cohen, S. B. Calderwood, G. K. Schoolnik, and A. Camilli.** 2002. Host-induced epidemic spread of the cholera bacterium. Nature **417:**642–645.
54. **Mey, A. R., E. E. Wyckoff, A. G. Oglesby, E. Rab, R. K. Taylor, and S. M. Payne.** 2002. Identification of the *Vibrio cholerae* enterobactin receptors VctA and IrgA: IrgA is not required for virulence. Infect. Immun. **70:**3419–3426.
55. **Mobley, H. L.** 1996. Virulence of *Proteus mirabilis*, p. 245–269. *In* J. W. Warren (ed.), Urinary tract infections: molecular pathogenesis and clinical management. ASM Press, Washington, D.C.
56. **Mobley, H. L., R. Belas, V. Lockatell, G. Chippendale, A. L. Trifillis, D. E. Johnson, and J. W. Warren.** 1996. Construction of a flagellum-negative mutant of *Proteus mirabilis*: effect on internalization by human renal epithelial cells and virulence in a mouse model of ascending urinary tract infection. Infect. Immun. **64:**5332–5340.
57. **Mobley, H. L., G. R. Chippendale, K. G. Swihart, and R. A. Welch.** 1991. Cytotoxicity of the HpmA hemolysin and urease of *Proteus mirabilis* and *Proteus vulgaris* against cultured human renal proximal tubular epithelial cells. Infect. Immun. **59:**2036–2042.
58. **Mobley, H. L., M. D. Island, and R. P. Hausinger.** 1995. Molecular biology of microbial ureases. Microbiol. Rev. **59:**451–480.
59. **Mobley, H. L., M. D. Island, and G. Massad.** 1994. Virulence determinants

of uropathogenic *Escherichia coli* and *Proteus mirabilis*. Kidney Int. Suppl. **47:**S129—S136.
60. **Mobley, H. L., and J. W. Warren.** 1987. Urease-positive bacteriuria and obstruction of long-term urinary catheters. J. Clin. Microbiol. **25:**2216–2217.
61. **Mouslim, C., D. A. Cano, A. Flores, and J. Casadesus.** 2000. Regulation of septation: a novel role for SerC/PdxF in *Salmonella*? Mol. Gen. Genet. **264:**184–192.
62. **Mulliez, E., M. Fontecave, J. Gaillard, and P. Reichard.** 1993. An iron-sulfur center and a free radical in the active anaerobic ribonucleotide reductase of *Escherichia coli*. J. Biol. Chem. **268:**2296–2299.
63. **Ninfa, A. J.** 1996. Regulation of gene transcription by extracellular stimuli, p. 1246–1262. *In* F. C. Neidhardt, R. Curtiss III, J. L. Ingraham, E. C. C. Lin, K. B. Low, B. Magasanik, W. S. Reznikoff, M. Riley, M. Schaechter, and H. E. Umbarger (ed.), *Escherichia coli* and *Salmonella*: cellular and molecular biology, vol. 1. American Society for Microbiology, Washington, D.C.
64. **Park, I. S., and R. P. Hausinger.** 1993. Site-directed mutagenesis of *Klebsiella aerogenes* urease: identification of histidine residues that appear to function in nickel ligation, substrate binding, and catalysis. Protein Sci. **2:**1034–1041.
65. **Peek, J. A., and R. K. Taylor.** 1992. Characterization of a periplasmic thiol: disulfide interchange protein required for the functional maturation of secreted virulence factors of *Vibrio cholerae*. Proc. Natl. Acad. Sci. **89:**6210–6214.
66. **Perry, R. D.** 1999. Signature-tagged mutagenesis and the hunt for virulence factors. Trends Microbiol **7**:385–388. (Discussion, **7:**388–389.)
67. **Pitout, J. D., K. S. Thomson, N. D. Hanson, A. F. Ehrhardt, E. S. Moland, and C. C. Sanders.** 1998. β-Lactamases responsible for resistance to expanded-spectrum cephalosporins in *Klebsiella pneumoniae*, *Escherichia coli*, and *Proteus mirabilis* isolates recovered in South Africa. Antimicrob. Agents. Chemother. **42:**1350–1354.
68. **Pittard, A. J.** 1996. Biosynthesis of the aromatic amino acids, p. 458–484. *In* F. C. Neidhardt, R. Curtiss III, J. L. Ingraham, E. C. C. Lin, K. B. Low, B. Magasanik, W. S. Reznikoff, M. Riley, M. Schaechter, and H. E. Umbarger (ed.), *Escherichia coli* and *Salmonella*: cellular and molecular biology, vol. 1. American Society for Microbiology, Washington, D.C.
69. **Poggio, S., C. Domeinzain, A. Osorio, and L. Camarena.** 2002. The nitrogen assimilation control (Nac) protein represses *asnC* and *asnA* transcription in *Escherichia coli*. FEMS Microbiol. Lett. **206:**151–156.
70. **Polissi, A., A. Pontiggia, G. Feger, M. Altieri, H. Mottl, L. Ferrari, and D. Simon.** 1998. Large-scale identification of virulence genes from *Streptococcus pneumoniae*. Infect. Immun. **66:**5620–5629.
71. **Rao, N. N., and A. Torriani.** 1990. Molecular aspects of phosphate transport in *Escherichia coli*. Mol. Microbiol. **4:**1083–1090.
72. **Reichard, P.** 1993. From RNA to DNA, why so many ribonucleotide reductases? Science **260:**1773–1777.
73. **Reichard, P.** 1988. Interactions between deoxyribonucleotide and DNA synthesis. Annu. Rev. Biochem. **57:**349–374.
74. **Reitzer, L. J.** 1996. Ammonia assimilation and biosynthesis of glutamine, glutamate, aspartate, asparagine, L-alanine, and D-alanine, p. 391–407. *In* F. C. Neidhardt, R. Curtiss III, J. L. Ingraham, E. C. C. Lin, K. B. Low, B. Magasanik, W. S. Reznikoff, M. Riley, M. Schaechter, and H. E. Umbarger (ed.), *Escherichia coli* and *Salmonella*: cellular and molecular biology, vol. 1. American Society for Microbiology, Washington, D.C.
75. **Rosenberg, H., R. G. Gerdes, and K. Chegwidden.** 1977. Two systems for the uptake of phosphate in *Escherichia coli*. J. Bacteriol. **131:**505–511.
76. **Schuster, S. C., R. V. Swanson, L. A. Alex, R. B. Bourret, and M. I. Simon.** 1993. Assembly and function of a quaternary signal transduction complex monitored by surface plasmon resonance. Nature **365:**343–347.
77. **Shimizu, T. S., N. Le Novere, M. D. Levin, A. J. Beavil, B. J. Sutton, and D. Bray.** 2000. Molecular model of a lattice of signalling proteins involved in bacterial chemotaxis. Nat. Cell Biol. **2:**792–796.
78. **Sprague, G. F., Jr., R. M. Bell, and J. E. Cronan, Jr.** 1975. A mutant of *Escherichia coli* auxotrophic for organic phosphates: evidence for two defects in inorganic phosphate transport. Mol. Gen. Genet. **143**:71–77.
79. **Sprinzl, M., C. Horn, M. Brown, A. Ioudovitch, and S. Steinberg.** 1998. Compilation of tRNA sequences and sequences of tRNA genes. Nucleic Acids Res. **26:**148–153.
80. **Struve, C., C. Forestier, and K. A. Krogfelt.** 2003. Application of a novel multi-screening signature-tagged mutagenesis assay for identification of *Klebsiella pneumoniae* genes essential in colonization and infection. Microbiology **149:**167–176.
81. **Sun, X., J. Harder, M. Krook, H. Jornvall, B. M. Sjoberg, and P. Reichard.** 1993. A possible glycine radical in anaerobic ribonucleotide reductase from *Escherichia coli*: nucleotide sequence of the cloned *nrdD* gene. Proc. Natl. Acad. Sci. **90:**577–581.
82. **Thulasiraman, P., S. M. Newton, J. Xu, K. N. Raymond, C. Mai, A. Hall, M. A. Montague, and P. E. Klebba.** 1998. Selectivity of ferric enterobactin binding and cooperativity of transport in gram-negative bacteria. J. Bacteriol. **180:**6689–6696.
83. **Tribe, D. E., H. Camakaris, and J. Pittard.** 1976. Constitutive and repressivle enzymes of the common pathway of aromatic biosynthesis in *Escherichia coli* K-12: regulation of enzyme synthesis at different growth rates. J. Bacteriol. **127:**1085–1097.
84. **Walker, K. E., S. Moghaddame-Jafari, C. V. Lockatell, D. Johnson, and R. Belas.** 1999. ZapA, the IgA-degrading metalloprotease of *Proteus mirabilis*, is a virulence factor expressed specifically in swarmer cells. Mol. Microbiol. **32:**825–836.
85. **Walsh, C. T., A. M. Gehring, P. H. Weinreb, L. E. Quadri, and R. S. Flugel.** 1997. Post-translational modification of polyketide and nonribosomal peptide synthases. Curr. Opin. Chem. Biol. **1:**309–315.
86. **Wanner, B. L.** 1996. Phosphorous assimilation and control of the phosphate regulon, p. 1357–1381. *In* F. C. Neidhardt, R. Curtiss III, J. L. Ingraham, E. C. C. Lin, K. B. Low, B. Magasanik, W. S. Reznikoff, M. Riley, M. Schaechter, and H. E. Umbarger (ed.), *Escherichia coli* and *Salmonella*: cellular and molecular biology, vol. 1. American Society for Microbiology, Washington, D.C.
87. **Warren, J. W., J. H. Tenney, J. M. Hoopes, H. L. Muncie, and W. C. Anthony.** 1982. A prospective microbiologic study of bacteriuria in patients with chronic indwelling urethral catheters. J. Infect. Dis. **146:**719–723.
88. **Webb, D. C., H. Rosenberg, and G. B. Cox.** 1992. Mutational analysis of the *Escherichia coli* phosphate-specific transport system, a member of the traffic ATPase (or ABC) family of membrane transporters. A role for proline residues in transmembrane helices. J. Biol. Chem. **267:**24661–24668.
89. **Weinberg, E. D.** 1978. Iron and infection. Microbiol. Rev. **42:**45–66.
90. **Welch, R. A., V. Burland, G. Plunkett, 3rd, P. Redford, P. Roesch, D. Rasko, E. L. Buckles, S. R. Liou, A. Boutin, J. Hackett, D. Stroud, G. F. Mayhew, D. J. Rose, S. Zhou, D. C. Schwartz, N. T. Perna, H. L. Mobley, M. S. Donnenberg, and F. R. Blattner.** 2002. Extensive mosaic structure revealed by the complete genome sequence of uropathogenic *Escherichia coli*. Proc. Natl. Acad. Sci. **99:**17020–17024.
91. **Willsky, G. R., R. L. Bennett, and M. H. Malamy.** 1973. Inorganic phosphate transport in *Escherichia coli*: involvement of two genes which play a role in alkaline phosphatase regulation. J. Bacteriol. **113:**529–539.
92. **Yu, J., H. Webb, and T. R. Hirst.** 1992. A homologue of the *Escherichia coli* DsbA protein involved in disulphide bond formation is required for enterotoxin biogenesis in *Vibrio cholerae*. Mol. Microbiol. **6:**1949–1958.
93. **Zhao, H., X. Li, D. E. Johnson, and H. L. Mobley.** 1999. Identification of protease and *rpoN*-associated genes of uropathogenic *Proteus mirabilis* by negative selection in a mouse model of ascending urinary tract infection. Microbiology **145:**185–195.

Editor: A. D. O'Brien